Transcriptional organization and regulation of the *Pseudomonas putida* flagellar system

Antonio Leal-Morales¶, Marta Pulido-Sánchez¶, Aroa López-Sánchez and Fernando Govantes*

Running title: Regulation of *P. putida* flagellar genes

Centro Andaluz de Biología del Desarrollo, Universidad Pablo de Olavide/Consejo Superior de Investigaciones Científicas/Junta de Andalucía and Departamento de Biología Molecular e Ingeniería Bioquímica, Universidad Pablo de Olavide, Sevilla, Spain.

*Corresponding author. Address: Centro Andaluz de Biología del Desarrollo, Universidad Pablo de Olavide, Carretera de Utrera, Km. 1, 41013, Sevilla, Spain. Phone: +34 954349386. Fax: +34 954349376. E-mail: fgovrom@upo.es

¶These authors contributed equally to the work presented

22 **ORIGINALITY-SIGNIFICANCE STATEMENT**

23 This is the first integrative study of the flagellar transcriptional cascade in
24 *Pseudomonas putida*. Our results provide a new transcriptional organization featuring
25 several operons with a nested architecture, detailed regulatory characterization of twenty-
26 two flagellar promoters and a novel hierarchy for the regulatory circuit of the flagellar
27 transcriptional cascade. The results presented represent a significant departure from
28 previous models for other related bacteria. High conservation of flagellar gene organization
29 and promoter sequences suggest that our observations may be relevant to other
30 pseudomonads.

31

SUMMARY

A single region of the *Pseudomonas putida* genome, designated the flagellar cluster, includes 59 genes potentially involved in the biogenesis and function of the flagellar system. Here we combine bioinformatics and *in vivo* gene expression analyses to clarify the transcriptional organization and regulation of the flagellar genes in the cluster. We have identified eleven flagellar operons and characterized twenty-two primary and internal promoter regions. Our results indicate that synthesis of the flagellar apparatus and core chemotaxis machinery is regulated by a three-tier cascade in which *fleQ* is a Class I gene, standing at the top of the transcriptional hierarchy. FleQ- and σ^{54}-dependent Class II genes encode most components of the flagellar structure, part of the chemotaxis machinery and multiple regulatory elements, including the flagellar σ factor FliA. FliA activation of Class III genes enables synthesis of the filament, one stator complex and completion of the chemotaxis apparatus. Accessory regulatory proteins and an intricate operon architecture add complexity to the regulation by providing feedback and feed-forward loops to the main circuit. Because of the high conservation of the gene arrangement and promoter motifs, we believe that the regulatory circuit presented here may also apply to other environmental pseudomonads.

INTRODUCTION

Motility allows bacterial cells to colonize new niches and escape from unfavourable habitats, minimizing the negative effects of competition and depletion of local resources (McDougald *et al*., 2012). For many bacteria, motility is directed by flagella, complex molecular machines that enable swimming of individual cells in liquid and semi-solid media and collective swarming on humid surfaces by engaging in propeller-like rotation driven by the proton-motive force (Altegoer *et al*., 2014; Kearns, 2010). The flagella-associated chemotaxis machinery, comprised of membrane-bound and cytosolic chemoreceptors and associated signal transduction proteins, promotes directional motion by controlling flagellar rotation in response to chemical gradients of attractants and repellents (Sourjik and Wingreen, 2012).

Bacterial flagella are proteinaceous appendages composed of over 30 different polypeptides (Altegoer *et al*., 2014). Flagella are constituted of three functional units: the basal body, a rotary machine embedded in the cell envelope; the filament, a long and thin helical appendage that protrudes from the cells and acts as a propeller; and the hook, a rigid, curved element that connects basal body and filament. The basal body is the most complex of these units. In Gram-negative bacteria, it is comprised of five separate components: (i) the MS-ring, an annular structure bound to the cell membrane, provides support to the complete flagellar architecture; (ii) attached to the MS-ring, the cytoplasmic C-ring is the flagellar rotor and the target for functional regulation by the chemotaxis machinery; (iii) a hollow rod anchored to the MS-ring spans the cell envelope, connecting the basal body with and transmitting rotation to the outer components of the flagella; (iv) the double LP ring is bound to the peptidoglycan and outer membrane and acts as bushings for smooth rotation of the rod; finally, (v) the in-built flagellar type III secretion system (FT3SS) provides the functions necessary for the export of flagellar proteins through the flagellum itself. Associated to the periphery of the flagellar basal body, the stator complex fuels flagellar rotation by coupling inward proton or sodium transport to the generation of torque

77 (Chevance and Hughes, 2008; Terashima *et al*., 2008). As documented thoroughly in
78 *Escherichia coli* and *Salmonella*, flagellar assembly is sequential, with the inner components
79 of the basal body being assembled first, followed by components of the rod, LP ring and
80 hook, which cannot be exported until the functional FT3SS is completed. Subsequent
81 assembly of the filament proteins is preceded by a shift in FT3SS specificity triggered by
82 completion of the hook structure. Finally, the accessory stator and chemotaxis complexes
83 are assembled. The structure and assembly of the flagella have been reviewed thoroughly
84 elsewhere (Altegoer *et al*., 2014; Chevance and Hughes, 2008; Evans *et al*., 2014).

85 Gram-negative bacteria differ with respect to the number of flagella, their distribution
86 across the surface and the transcriptional organization and regulation of the flagellar genes.
87 Although flagellar genes are scattered in the genomes of some organisms, most often they
88 are grouped in one or a few genomic regions (Smith and Hoover, 2009). *Pseudomonas*
89 *putida* is a well-studied soil bacterium endowed with extraordinary metabolic versatility that
90 has become a model organism for biodegradation of organic toxicants and an attractive
91 platform for biofilm-based industrial applications (Gross *et al*., 2007; Li *et al*., 2007; Martins
92 Dos Santos *et al*., 2004). *P. putida* shows lophotrichous flagellation, consisting of a tuft of 5
93 to 7 flagella at a single pole (Harwood *et al*., 1989). In the reference strain KT2440, most
94 structural components of the flagella, the core chemotaxis signal transduction system and a
95 number of dedicated regulatory proteins are encoded in a ~70 kbp chromosomal region
96 known as the flagellar cluster (**Fig. 1A**). Additional genes encoding a second stator complex
97 (Toutain *et al*., 2005), several paralogs of the core chemotaxis components (García-Fontana
98 *et al*., 2013) and a set of 27 chemoreceptors (Corral-Lugo *et al*., 2016) are scattered
99 elsewhere in the genome.

100 The biosynthesis of bacterial flagella is a complex and ordered process that mirrors
101 the assembly sequence (Smith and Hoover, 2009). In order to achieve the correct temporal
102 regulation of flagellar genes so that the structural protein are produced as they are required
103 for assembly of the nascent flagellum, bacteria use hierarchically organized regulatory

104 circuits in the form of a transcriptional cascades (Smith and Hoover, 2009). Little is known
105 about the transcriptional organization and regulation of the flagellar genes in most members
106 of the genus *Pseudomonas*, and much of it has been extrapolated from the transcriptional
107 cascade of *Pseudomonas aeruginosa* described in the seminal work of Dasgupta *et al*.
108 (2003). In this organism, the flagellar genes are organized into four classes to reflect the
109 timing of their expression and the transcription factors involved in their regulation. Class I
110 genes, encoding the master regulator FleQ and the flagellar σ factor FliA, stand at the top
111 of the hierarchy and are not regulated by any of the dedicated flagellar transcription factors.
112 Class II genes encode the cytoplasmic and membrane-bound components of the basal
113 body, the FT3SS, the two-component system FleSR and the auxiliary regulatory proteins
114 FleN and FlhF, involved in control of the number and polar location of the flagella,
115 respectively. Genes in this class are activated by FleQ in a σ^{54}-dependent fashion. Class III
116 genes encode the structural components of the rod, the outer LP ring and the hook, and
117 their expression is also σ^{54}-dependent and activated by FleR. Finally, Class IV genes,
118 encoding the filament proteins, the core components of the chemotaxis apparatus and the
119 stator complex are dependent on the flagellar σ factor FliA. In *P. aeruginosa* FleQ activation
120 of the Class II genes is antagonized by the auxiliary protein FleN and the second messenger
121 c-di-GMP (Dasgupta *et al*., 2000). The histidine kinase FleS likely activates the response
122 regulator FleR by phosphorylation (Dasgupta *et al*., 2003), although the involvement of FleS
123 in flagellar gene regulation has recently been questioned (Zhou *et al*., 2021) and the signals
124 and relevant conditions have not yet been explored. FliA sequestration by the anti-σ factor
125 FlgM prevents premature activation of the Class IV promoters (Dasgupta *et al*., 2003; Frisk
126 *et al*., 2002). FliA inhibition is likely released by FlgM secretion through the FT3SS upon
127 completion of the hook, as shown first in *Salmonella* (Karlinsey *et al*., 2000), although
128 experimental evidence of this phenomenon in *P. aeruginosa* is still lacking. In addition, the
129 anti-σ factor antagonist HsbA has been shown to prevent FlgM inhibition by a partner-

130 switching mechanism. HsbA activity is in turn regulated by HsbR and HptB in response to
131 as of yet unknown signals (Bhuwan *et al*., 2012). The *P. aeruginosa* flagellar system and its
132 regulation was reviewed recently (Bouteiller *et al*., 2021).

133 The *P. putida* KT2440 genome encodes all the known elements shown to be involved
134 in flagellar regulation in *P. aeruginosa*, and previous work from our group and others has
135 confirmed the role of FleQ as the master regulator of the flagellar cascade and the role of
136 the σ factor FliA activating the expression of some late flagellar genes (Blanco-Romero *et*
137 *al*., 2018; Jiménez-Fernández *et al*., 2016; Rodríguez-Herva *et al*., 2010; Wang *et al*., 2018).
138 Recently, ChIP-seq studies suggested that FleQ may bind *in vivo* upstream from genes
139 encoding components of the basal body (FlhA, FlhB, FlgA, FlgB, FlgF, FlgG), the hook (FliE,
140 FliK), the motor protein MotB, the anti-σ factor FlgM and some chemotaxis elements (CheV,
141 PP2310, PP4888) (Blanco-Romero *et al*., 2018), but the outcome of such interaction in
142 terms of transcriptional regulation has not been explored. Our recent work has clarified the
143 transcriptional organization, promoter arrangement and regulation of the *flgAMNZ* and
144 *flhAF-fleN-fliA* operons (Navarrete *et al*., 2019; Wirebrand *et al*., 2018). Although an
145 integrated model of the *P. putida* flagellar cascade comparable to that of *P. aeruginosa* is
146 as of yet unavailable, the preliminary work suggests significant differences in the
147 transcriptional organization and regulation of the flagellar genes between both species.
148 Significantly, the flagellar/chemotaxis system of *P. putida* and other so-called environmental
149 *Pseudomonas* differs from *P. aeruginosa* in the type of flagellation (lophotrichous *vs.*
150 monotrichous) the identity and functionality of the chemoreceptors. These differences may
151 correlate with the different requirements of the *P. aeruginosa* pathogenic lifestyle *vs.* the
152 free living soil/saprophytic lifestyle of *P. putida* (Lacal *et al*., 2013; Matilla *et al*., 2021;
153 Sampedro *et al*., 2015)

154 The present study clarifies the transcriptional organization of the flagellar cluster and
155 the regulatory circuit controlling flagellar synthesis in *P. putida*. Our results support a
156 transcriptional circuit in which the temporal regulation of the flagellar components is

157 achieved by the combination of a three-tier transcriptional cascade and several feedback
158 and feed-forward loops to fine-tune gene expression according to the assembly status and
159 relevant physiological and environmental cues.
160

161 **RESULTS**

162 **A cluster of 59 flagella-related genes is highly conserved in *Pseudomonas* spp.**

163 In order to identify the complete set of genes related to flagellar motility and chemotaxis
164 within the flagellar cluster, we have revised the annotation in the light of recent experimental
165 evidence. ORF PP_4328 encodes a protein of unknown function containing the domain
166 designated "flagellar hook-length control-like, C-terminal" (InterPro accession: IPR021136),
167 found in the hook length control protein FliK. Transcription from the upstream promoter
168 region is dependent on the flagellar σ factor FliA in *P. putida* (Jiménez-Fernández *et al*.,
169 2016). Accordingly, we have designated this ORF *fliK2*. The ORF immediately downstream,
170 PP_4329, is an ortholog of *flhX*, a gene identified in several bacterial genomes whose
171 product resembles the C-terminal domain of the FT3SS protein FlhB (Pallen *et al*., 2005). A
172 function of FlhX as a partial replacement for FlhB function has been documented in
173 *Helicobacter pylori* (Smith *et al*., 2009; Wand *et al*., 2006). The *P. putida* PP_4329 product
174 bears 34% identity and 56% similarity to that of HP:1575, its *H. pylori* counterpart. PP_4331
175 encodes an ortholog of *Vibrio cholerae* FlrD, an auxiliary protein to transcriptional regulation
176 by FlrBC, the *V. cholerae* counterparts of *Pseudomonas* FleSR (Moisi *et al*., 2009). Similarly,
177 PP_4333 and PP_4334 encode orthologs of the *Vibrio* spp. ParP and ParC proteins,
178 required for polar localization of the chemotaxis complexes (Ringgaard *et al*., 2018).
179 Sequence alignments revealed 32%, 44% and 51% identity and 53%, 63% and 70%
180 similarity between the PP_4331, PP_4333 and PP_4334 products and the products of their
181 *V. cholerae* El Tor strain ATCC 39315 orthologs, VC_2058, VC_2060 and VC_2061. Finally,
182 PP_4362, PP_4363 and PP_4364 encode orthologs of *P. aeruginosa* HptB, HsbR and
183 HsbA, involved, along with the anti-sigma factor FlgM, in posttranslational regulation of FliA
184 (Bhuwan *et al*., 2012). Sequence alignments showed 51%, 62% and 64% identity and 66%,
185 74% and 79% similarity between the products of PP_4362, PP_4363 and PP_4364 and their
186 *P. aeruginosa* PAO1 counterparts PA_3345, PA_3346 and PA_3347 Our results suggest
187 that at least 59 of the genes present in the cluster are potentially related to the flagellar

188 function (**Fig. 1A; Supplementary Table S1**). In contrast, we have been unable to establish
189 such functional relationship for the seven consecutive ORFs (PP_4345 to PP_4350 and
190 PP_5673) with unusually low G+C content located upstream from *flhA*, and the single ORFs
191 PP_4330, PP_4379 and PP_4387 (**Fig. 1A**).

192 We have examined the conservation of the flagellar cluster in 550 genomes available
193 online at the *Pseudomonas* Genome Database (Winsor *et al*., 2016); available at
194 pseudomonas.com). Precomputed ortholog analyses revealed that 51 of the genes were
195 conserved in all the genomes analyzed, 7 were conserved in over 90% of the genomes, and
196 a single gene, *fliT,* for which members of two separate ortholog groups were found, was
197 conserved in 80% of the genomes. High conservation of the 59-gene set likely suggests that
198 it encodes an integral part of the flagellar apparatus in the vast majority of members of the
199 genus *Pseudomonas*. Synteny analysis performed on 401 of the genomes revealed nearly
200 universal conservation of the gene order and orientation of the flagellar cluster, with very
201 few exceptions (complete analysis in **Supplementary File S1**). Based on the chromosomal
202 location of the flagellar cluster genes, we have defined four groups encompassing most of
203 the genomes analyzed (**Fig. 1B; Supplementary File S1**). In Group I, including multiple *P.*
204 *putida* and *Pseudomonas syringae* strains among others, all genes are found in a single
205 chromosomal region in the same order and orientation as in *P. putida* KT2440. Group II,
206 including strains of *Pseudomonas fluorescens* and related species, bears the flagellar
207 cluster split in two separate regions, with the split point between *flgF* and *flgE*. Exceptionally,
208 the *fliK2-flhX* gene pair was not linked to the cluster in some members of groups I and II
209 (e.g., *P. syringae* and *Pseudomonas savastanoi* strains). In Group III, which includes most
210 *Pseudomonas stutzeri* strains examined, the cluster is disrupted between *fliC* and *flgL*, and
211 in ~70% of the cases, also between *fleQ* and *fliT*, resulting in the location of their flagellar
212 clusters in two or three separate chromosomal regions. Finally, Group IV, encompassing
213 most *P. aeruginosa* strains, displays the only major disruption in the synteny of the cluster:
214 the genes *hptB*, *hsbR* and *hsbA* are found downstream from *cheR* in one chromosomal

215 location, while segments containing *fliK2* to *fliK* and *fliJ* to *flgB* are located in two additional
216 chromosomal regions. A similar analysis revealed that orthologs of *motA* and *motB*, the only
217 structural flagellar genes not linked to the *P. putida* flagellar cluster, are present in nearly all
218 the *Pseudomonas* genomes analyzed, in a separate chromosomal location, in the order
219 *motAB*, and almost invariably linked to the gene *rsgA* and the orthologs of the KT2440 ORF
220 PP_4906 (**Supplementary File S1**).

221 Flagellar clusters generally include additional genes; some are related to covalent
222 modification of the flagella or are the result of duplication of specific genes in the cluster (
223 Dasgupta *et al*., 2003), while others appear unrelated to flagellar function. Synteny analysis
224 also revealed that insertion of additional genes occurs preferentially at some of the split
225 points noted above (*flhB2-flrD*, *hsbA-fliJ*, *fliC-flgL*, *flgF-flgE* and *flgB-cheR*), along with the
226 *flhA-flhB* and (less commonly) the *fliE-fleR* intergenic region (**Fig. 1B; Supplementary File**
227 **S1**).

228 Taken together, the results of our analysis suggest that *Pseudomonas* genomes have
229 evolved to preserve the sequence and organization of a set of 59 genes related to the
230 flagellar function. Accordingly, most genes in the cluster are found in the same genomic
231 neighborhood in all the genomes analyzed, and disruption of synteny occurs almost
232 exclusively in a few specific locations.

233 **Transcriptional organization of the *P. putida* KT2440 flagellar cluster**

234 As a first approach to the identification of the transcriptional units present at the
235 KT2440 flagellar cluster, we analyzed the coverage obtained in a strand-specific RNA-seq
236 experiment (**Fig. 2A, C and E**). We observed continuous, uninterrupted strand-specific
237 transcription, as expected for genes co-transcribed as an operon, in ten regions containing
238 flagellar genes within the cluster: *fliK2-flhB2* and *flgAMNZ* at the top strand, and *flhAF-fleN-*
239 *fliA-cheYZAB-motCD-parCP-cheW-flrD*, *hsbAR-hptB-fliKLMNOPQR-flhB*, *fliHIJ*, *fliEFG*,
240 *fliC-flaG-fliDST-fleQSR*, *flgFGHIJKL*, *flgBCDE-pp4387*, and *cheV-cheR* at the bottom
241 strand. Continuous bottom strand transcription was also observed at a region spanning

242 *motA* and *motB* (**Supplementary Fig. S1**). Since the neighboring genes are transcribed
243 from the top strand, these results suggest that *motA* and *motB* are co-transcribed as a
244 bicistronic operon.

245 In contrast to our RNA-seq results, the fourteen-gene string running from *flhA* to *flrD* is
246 broken into seven separate transcriptional units in *P. aeruginosa* (Dasgupta *et al*., 2003).
247 On the other hand, our recent work showed that at least *flhA*, *flhF*, *fleN* and *fliA* are part of
248 the same operon in *P. putida* (Navarrete *et al*., 2019). To test the validity of the transcriptional
249 organization inferred from the RNA-seq data, we performed RT-PCR with oligonucleotides
250 framing all intergenic regions larger than 3 bp from *flhA* to *flrD* and cDNA from *P. putida*
251 KT2442, a rifampicin-resistant derivative of KT2440, as a template (**Fig. 2B**). Amplification
252 was obtained from all of the intergenic regions tested, strongly suggesting that transcripts
253 initiated from P*flhA* span all fourteen coding regions down to *flrD*. This assay was also
254 performed with cDNA from MRB49, a KT2442 derivative bearing a polar miniTn*5*-Km
255 insertion in *flhF* (Navarrete *et al*., 2019). Transcription levels were diminished for all
256 intergenic regions downstream from the insertion down to *motD-parC*. Polarity was not
257 observed at the *parP-cheW* and *cheW-flrD* junctions. The loss of the polar effect in this
258 region and the increased transcription obtained in both the wild-type and mutant strain,
259 suggest the presence of an internal promoter activity. We note that one or more FliA-
260 dependent internal promoters may be present in this region and not be detected in this
261 background, as polarity of the *flhF*::miniTn*5*-Km mutation renders this strain FliA$^-$ (Navarrete
262 *et al*., 2019).

263 Discrepancy with the transcriptional organization proposed for *P. aeruginosa* was also
264 observed at the regions spanning from *hptB* to *fliL*, *fliE* to *fliJ*, *fliC* to *fleR* and *flgA* to *flgZ*.
265 RT-PCR assays using KT2442 cDNA as a template and primers spanning the conflicting
266 intergenic regions confirmed co-transcription of *hptB*, *fliK* and *fliL* (**Fig.2D**) and *fliD*, *flaG*,
267 *fliD*, *fliS*, *fliT*, *fleQ* and *fleS* (**Fig. 2F**), and transcriptional termination at the *fliG-fliH* intergenic
268 region (**Fig. 2D**), consistent with the RNA-seq results. A similar RT-PCR analysis of the

269 *flgAMNZ* operon was previously published (Wirebrand *et al*., 2018). Altogether, the RNA-
270 seq and RT-PCR data and our previously published results (Navarrete *et al*., 2019;
271 Wirebrand *et al*., 2018) strongly suggest that the flagellar genes of the *P. putida* KT2440
272 flagellar cluster are transcribed as ten separate operons. In addition, at least two of the
273 operons contain internal promoters. Finally, an eleventh flagellar operon not linked to the
274 cluster spans the genes *motA* and *motB*.

275 ***P. putida* flagellar promoters revealed by sequence alignment**

276 Given the high conservation of the flagellar cluster organization across the genus
277 *Pseudomonas*, we hypothesized that such conservation may also extend to the promoter
278 regions preceding each of the operons. To test this hypothesis, we performed sequence
279 alignments of the intergenic regions upstream from *fliK2*, *flhA*, *hsbA*, *fliH*, *fliE*, *fliC*, *flgF*, *flgB*,
280 *cheV*, *flgA* and *motA*, all of which are expected to bear the primary promoters for the operons
281 defined above. For this purpose, we used the genomic sequences of *P. putida* strains
282 KT2440 and F1, *P. syringae* pv tomato strain DC3000, *P. syringae* pv syringae strain B728a,
283 *P. savastanoi* pv phaseolicola strain 1448a, *P. fluorescens* strain SBW25 and *Pseudomonas*
284 *protegens* strain Pf5 (**Fig. 3, Supplementary Fig. S2; Supplementary File S2**). While the
285 general conservation of the intergenic sequences was modest, alignments revealed
286 conserved motifs showing high similarity to the σ^{54}-dependent promoter consensus (Barrios
287 *et al*., 1999) at the intergenic regions upstream from *flhA*, *fliE*, *flgF*, *flgB* and *flgA*. We also
288 found conserved sequences bearing similar to the FliA-dependent promoter consensus
289 sequence (Rodríguez-Herva *et al*., 2010) upstream from *fliK2*, *fliC* and *cheV*, the latter
290 located within the divergent *flgA* coding sequence. A motif resembling the σ^{70}-dependent
291 promoter consensus featuring an extended -10 and a poor -35 box (Bown *et al*., 1997) was
292 present upstream from *hsbA*. We observed that the intergenic region upstream from *fliH* was
293 too short to accommodate a promoter (<15 bp) in the *P. fluorescens*, *P. protegens*, *P.*
294 *syringae* and *P. savastanoi* strains used in the alignment. A survey of *P. putida* strains
295 revealed generally longer intergenic regions containing two copies of a repetitive extragenic

296 palindromic sequence previously documented (Aranda-Olmedo *et al*., 2002), but no obvious
297 similarity to known promoter consensus motifs. Yet, as our RNA-seq and RT-PCR results
298 predict that a promoter must be active upstream from *fliH*, we included this region in the
299 analyses below.

300 Because we have previously shown evidence of the presence of additional promoter
301 activities upstream of *flhF*, *fliS* and *flgM* (Jiménez-Fernández *et al*., 2016; Navarrete *et al*.,
302 2019; Wirebrand *et al*., 2018), we also assessed the presence of putative promoter motifs
303 by means of sequence alignment in multiple additional intergenic regions of the flagellar
304 cluster (**Fig. 3, Supplementary Fig. S2; Supplementary File S2**). Additional matches to
305 the σ^{54}-dependent promoter consensus were identified at the intergenic regions upstream
306 from *fliL*, *fliK* and *fleS*, while sequences showing conservation at the -24 but not the -12 motif
307 were found upstream from *fliD and flgZ*. We also identified conserved sequences matching
308 the FliA-dependent promoter consensus upstream from *fliS* and *flgM*, and a putative σ^{70}-
309 dependent promoter motif upstream from *fleQ*. Finally, putative internal promoters located
310 within the coding sequences of the preceding genes were also found upstream from *parC*
311 and *flhF* (σ^{54}-dependent), and *cheA* (FliA-dependent). In summary, this analysis revealed
312 twenty-one putative flagellar promoters. Twelve such regions bear matches to the σ^{54}
313 consensus, seven show similarity with the FliA consensus, and two more harbor putative
314 σ^{70} promoter motifs.

315 **Strategy for analysis of the regulation of the *P. putida* flagellar cluster promoters**

316 In order to characterize the expression from the putative flagellar promoters identified,
317 we expanded our pre-existing collection of *P. putida* promoter fusions (Jiménez-Fernández
318 *et al*., 2016) to include all the potential promoter regions identified. The selected regions
319 were cloned into the Gateway® vectors pMRB2 or pMRB3 to generate transcriptional fusions
320 to the reporters *gfp*-mut3 and *lacZ*, as previously described (Jiménez-Fernández *et al*.,
321 2016). All twenty-two *gfp-lacZ* fusion plasmids and the empty vector control pMRB1 were

322 transferred to selected *P. putida* strains by mating. Expression was subsequently monitored
323 along the growth curve by means of A_{600} and GFP fluorescence measurements in a
324 microtiter plate reader with temperature and shaking control capabilities. GFP fluorescence
325 was plotted *vs* A_{600} and differential rates of GFP accumulation during exponential growth
326 (d*fluorescence*/dA_{600}) were calculated from the slope of the linear fit of the plotted data
327 (Jacob and Monod, 1961) (**Supplementary Fig. S3**). The results of thiese experiments are
328 summarized in **Supplemental File S3**.

329 To assess the effect of different regulatory factors on flagellar/chemotaxis promoter
330 transcription we used a subtractive approach in which we compared activity of the gene
331 fusion constructs in the wild-type strain with that in mutants bearing deletions of single
332 regulatory genes in an otherwise wild-type background. To this end, we chose the wild-type
333 *P. putida* strain KT2442 and its mutant derivatives MRB52, MRB149, MRB71 and MRB93,
334 bearing in-frame deletions of the *fleQ*, *rpoN*, *fleN* and *fleR* regulatory genes, respectively.
335 To assess whether the observed regulatory effects are direct or indirect, we used an additive
336 strategy. To this end, we constructed MRB130, a *P. putida* KT2442 derivative lacking the
337 flagellar cluster (Δflagella), including all the regulatory elements therein. In this background,
338 we inserted miniTn*7* derivatives expressing regulatory elements ectopically to test their
339 effect on the expression of the fusion constructs of the flagellar/chemotaxis predicted
340 promoter regions in the absence of other components of the flagellar cascade. In this
341 context, we interpreted restoration of expression in the presence of FleQ or FliA as evidence
342 of direct interaction between each regulatory factor and the cognate promoter region.

343 **P*fleQ* and P*fliH* transcription is not regulated by FleQ, FleR or FliA.**

344 The differential rates of GFP accumulation from the P*fleQ-gfp-lacZ* and P*fliH-gfp-lacZ*
345 fusions were low (4.06±0.30 and 5.45±0.26 arbitrary units, respectively) and
346 indistinguishable from to the empty vector values (3.88±0.42 arbitrary units). As an
347 alternative approach, expression was monitored by end-point β-galactosidase assays in
348 exponential and stationary phase. Expression from both promoters was negligible in

349 exponential phase, but the activity levels were significantly increased (4- to 5-fold) in
350 stationary phase (**Fig. 4**). P*fliH* transcription was not significantly altered in strains lacking
351 the transcription factors FleQ and FleR, or the auxiliary regulatory protein FleN. In the case
352 of P*fleQ*, statistically significant changes in GFP accumulation were observed in the Δ*fleQ*,
353 Δ*fleN* and Δ*fleR* mutants in stationary phase, but the extent of the regulation (1.2-fold or
354 less) suggests that these differences may be due to minor changes is cell physiology rather
355 than the result of a true regulatory process. Using the additive approach we noted that the
356 differential rates derived from the P*fleQ* fusion were 2-fold lower in the Δflagella strain in
357 stationary phase. However, the wild-type expression levels were not restored by ectopic
358 production of FleQ or FliA (**Fig. 4A**). P*fliH* expression was not affected by the deletion of the
359 complete flagellar cluster or the ectopic production of FliA (**Fig. 4B**). Taken together, these
360 results suggest that the upstream regions of *fleQ* and *fliH* contain promoters that are poorly
361 expressed in exponential phase, induced in stationary phase, and not substantially
362 regulated by any of the known flagellar transcription factors.

363 **Flagellar promoters directly regulated by FleQ**

364 Analysis of the differential rates of GFP accumulation showed that all twenty additional
365 flagellar promoters drove significant levels of transcription from the fusion constructs (**Figs.**
366 **5 and 6)**. Fifteen of these fusions were clearly downregulated (2- to 41-fold) in the Δ*fleQ*
367 strain, suggesting the direct or indirect involvement of FleQ in their regulation. Statistically
368 significant regulation below the 2-fold threshold was also observed for the weakly active
369 P*fliK*, P*fliD* and P*flgZ* promoter regions, and for P*flhF* and P*hsbA*, which showed relatively
370 high levels of FleQ-independent expression. Taken together, our results are fully consistent
371 with the notion that FleQ is the master activator of the synthesis of the vast majority of
372 flagellar and chemotaxis components.

373 To identify which flagellar promoters are directly regulated by FleQ, we tested the
374 expression of the set of FleQ-activated promoter fusions in the Δflagella strain bearing
375 miniTn*7-nahR*-P*sal-fleQ*, which produces FleQ ectopically from the salicylate-inducible P*sal*

376 promoter (**Figs. 5 and 6**). Preliminary assays showed that salicylate induction greatly
377 decreased the growth rate and was not used in these experiments. Nevertheless, *fleQ*
378 transcription from uninduced P*sal* was still evident in RT-PCR assays (**Supplementary Fig.**
379 **S4**), and ectopic production of FleQ in these conditions was sufficient to cause a significant
380 increase in the differential expression rates (2- to 110-fold) obtained from the P*parC*, P*flhF*,
381 P*flhA*, P*fliL*, P*fliK*, P*fliE*, P*fleS*, P*fliD*, P*flgF*, P*flgB*, P*flgA* and P*flgZ* promoter fusions.
382 Significantly, the sequence alignment study of these twelve promoter regions revealed the
383 presence of putative σ^{54}-dependent promoter motifs (**Fig. 3, Supplementary Fig. S2;**
384 **Supplementary File S2**). In addition, putative FleQ binding sites bearing similarity to the
385 consensus sequences proposed for *P. aeruginosa* (Baraquet and Harwood, 2015) and *P.*
386 *putida* (Molina-Henares *et al*., 2016) were found either upstream or downstream from the
387 σ^{54}-binding motifs (**Supplementary Fig. S5**). Still, it may be argued that FleQ regulation
388 may conceivably be indirect in the Δflagella background, as recent ChIP-Seq results suggest
389 that FleQ may bind DNA in the vicinity of some regulatory genes outside of the flagellar
390 cluster (Blanco-Romero *et al*., 2018). We have previously shown that P*flhA*, P*flgA* and P*flgB*
391 are still activated by FleQ when expressed in *E. coli*, an organism that naturally lacks FleQ
392 and uses a completely different strategy to regulate flagellar gene expression (Jiménez-
393 Fernández *et al*., 2016). To clarify this issue, we expanded these results by assessing
394 expression of the twelve promoter fusion set in *E. coli* ET8000 producing *P. putida* FleQ
395 from its own promoter region at the multicopy plasmid pMRB99 (**Supplementary Table S2**).
396 Ten of the twelve promoters were significantly activated in a FleQ-dependent fashion in this
397 background, with induction ratios ranging from 4- to 81-fold. In contrast, P*fleS* and P*flgZ*
398 expression was not significantly altered by the presence of FleQ. These results suggest that
399 FleQ interacts directly at least with the P*parC*, P*flhF*, P*flhA*, P*fliL*, P*fliK*, P*fliE*, P*fliD*, P*flgF*,
400 P*flgB* and P*flgA* promoter regions to activate transcription, while the direct involvement of
401 FleQ in activation of the P*fleS* and the P*flgZ* is at this point unclear (also see below).
402 Expression from the vast majority fusions in this set showed significantly reduced expression

403 in a Δ*rpoN* background lacking σ^{54} (**Fig. 5**). However, the induction ratio was low (less than
404 2-fold) for P*fliK*, P*fleS* and P*fliD* promoters, and the difference was not statistically significant
405 for P*fliD.* To investigate the involvement of σ^{54} further and explore a possible effect of the
406 growth phase on σ^{54} regulation of the flagellar promoters, we also assayed expression by
407 means of end-point β-galactosidase assays in wild-type and Δ*rpoN P. putida* strains grown
408 to exponential and stationary phase (**Supplementary Table S3**). Statistically significant
409 differences in the measured activity with induction ratios of 2-fold or more were observed
410 with all promoters in stationary phase and all promoters but P*fleS* and P*flgZ* in exponential
411 phase, suggesting that σ^{54} contributes to the expression of all twelve promoters and its effect
412 on P*fleS* and P*flgZ* is more prominent in stationary phase.

413 Expression from the twelve promoter fusion set was also measured in a KT2442
414 derivative lacking the auxiliary regulatory protein FleN (**Fig. 5**). The differencial fluorescence
415 accumulation rates were clearly increased for eleven of the twelve fusions (2- to 13-fold) in
416 the Δ*fleN* background. Exceptionally, a small (less than 2-fold) but statistically significant
417 increase was observed for the weak P*flgZ* promoter. These results support the notion that
418 FleN antagonizes FleQ activation of the flagellar promoters (Dasgupta and Ramphal, 2001).
419 The second messenger c-di-GMP has been shown to positively and negatively modulate
420 FleQ activity (Baraquet *et al*., 2012; Claudine and Harwood, 2013; Hickman and Harwood,
421 2008). We also tested expression of the twelve fusions in *P. putida* strains that produce the
422 *Caulobacter crescentus* diguanylate cyclase PleD* or the *E. coli* phosphodiesterase YhjH
423 ectopically, thus increasing or decreasing the intracellular c-di-GMP concentrations. To this
424 end, we chose a KT2442 derivative lacking the high molecular weight adhesin LapA, as c-
425 di-GMP overproduction provokes aggregation of LapA$^+$ *P. putida* (Jiménez-Fernández *et al*.,
426 2016) that precludes accurate absorbance and fluorescence measurements. The differential
427 rates of fluorescence accumulation in the unmodified *lapA*$^-$ strain were generally similar to
428 the strain with artificially decreased c-di-GMP levels, suggesting that c-di-GMP levels are

429 generally low in our experimental conditions. Comparison of the *P. putida* strains bearing
430 modifed c-di-GMP levels showed statistically significant c-di-GMP-dependent
431 downregulation of the twelve fusions, with inhibition ratios of 2- to 21-fold, except for a
432 somewhat smaller (1.8-fold) ratio obtained with the P*fliK* fusion (**Fig. 5**). Taken together, our
433 results indicate that the P*parC*, P*flhF*, *flhA*, P*fliL*, P*fliK*, P*fliE*, P*fliD*, P*flgF*, P*flgB* and P*flgA*
434 promoters are dependent on the alternative σ factor σ^{54}, positively regulated by FleQ,
435 negatively regulated by FleN and inhibited by high c-di-GMP levels. Although we have not
436 been able to demonstrate the direct regulation of P*fleS* by FleQ beyond any doubt, the
437 weight of the bioinformatic and experimental evidence and the coincidence of its behavior
438 with the rest of the set in every other regard strongly suggests that P*fleS* is likely a *bona fide*
439 FleQ-dependent promoter. On the other hand, P*flgZ*, a poorly expressed promoter, exhibited
440 a similar response to FleQ, FleN, σ^{54} and c-di-GMP, but the extent of the regulation was
441 modest in all cases.

442 **FleR is not essential for flagellar function and flagellar gene expression**

443 The FleSR two-component system is responsible for the activation of Class III flagellar
444 genes in *P. aeruginosa* and other bacteria (Dasgupta *et al*., 2003; Echazarreta and Klose,
445 2019), but is not characterized in *P. putida*. To explore a possible function of FleSR in
446 flagellar motility and the regulation of the flagellar cluster, we constructed MRB92 and
447 MRB93, two KT2442 derivatives bearing in-frame deletions of *fleS* and *fleR*, respectively.
448 Swimming assays were performed with the Δ*fleR* and Δ*fleS* mutant using the wild-type and
449 Δ*fleQ* strains as positive and negative controls, respectively. The sizes of the swimming
450 halos produced by the wild-type, Δ*fleR* and Δ*fleS* strains were indistinguishable, while no
451 motility halo was obtained with the Δ*fleQ* mutant (**Supplementary Fig. S6**). These results
452 indicate that FleR and FleS are not essential for flagellar motility, at least under our
453 experimental conditions.

454 To determine the contribution of FleR to the regulation of the flagellar promoters,
455 expression from the complete fusion set was also examined in the Δ*fleR* mutant (**Figs. 5**

456 **and 6**). Deletion of *fleR* had a statistically significant effect on the differential rates of
457 fluorescence accumulaion by the P*cheA*, P*flhF*, P*flhA*, P*fliL*, P*hsbA*, P*fleS*, P*fliS*, P*fliD*, P*fliC*,
458 P*flgF*, P*flgB*, P*flgA*, P*flgM* and P*motA* promoters. However, the fold changes were modest
459 in all cases, except for 2-fold downregulation of the FleQ-dependent P*flgF* and P*flgB* and 2-
460 fold upregulation of P*fliC*. These results suggest that FleR does not have a major role in the
461 regulation of flagellar gene expression, but may contribute to fine-tune the expression of
462 some flagellar operons. Alternatively, FleR function may involve a signaling event that does
463 not occur under our experimental conditions.

464 **Flagellar promoters directly regulated by FliA**

465 The additive approach was also used to assess which promoters of the flagellar cluster
466 are directly regulated by the flagellar σ factor FliA. To this end, differential rates of
467 fluorescence accumulation were assessed for the complete set of FleQ-regulated flagellar
468 promoters in the Δflagella strain bearing miniTn*7-nahR*-P*sal-fliA*, which produces FliA
469 ectopically from the salicylate-inducible P*sal* promoter. As with the FleQ-producing construct
470 above, salicylate induction was detrimental to growth, but in the absence of salicylate,
471 ectopic production of FliA significantly stimulated expression (4- to 33-fold) from all seven
472 promoter regions (namely P*fliK2*, P*cheA*, P*fliS*, P*fliC*, P*cheV*, P*flgM* and P*motA*) bearing
473 matches to the FliA consensus sequence (**Fig. 6**). In contrast, ectopic production of FleQ
474 failed to significantly alter the expression from any of these fusions, except for a modest (~2-
475 fold) increase in P*fliK2* (**Fig. 6**). Conversely, ectopic production of FliA had no significant
476 effect on the differential rates of fluorescence accumulation by the FleQ-dependent P*flhA*,
477 P*fliK*, P*fleS*, and P*flgF*, while statistically significant but modest (≤2-fold) stimulation was
478 observed with P*parC*, P*flhF*, P*fliL*, P*fliE*, P*fliD*, P*flgB*, P*flgA* and P*flgZ* (**Fig. 5**). Although most
479 FliA-dependent fusions were downregulated in the Δ*fleQ*, Δ*rpoN* and Δ*fleN* backgrounds,
480 we note that P*fliC* expression was increased in the absence of FleN (**Fig. 6**). Taken together,
481 our results suggest that the promoters contained at the P*fliK2*, P*cheA*, P*fliS*, P*fliC*, P*cheV*,
482 P*flgM* and *motA* promoter regions are dependent on the alternative σ factor FliA, and

483 indirectly regulated by σ^{54} and FleQ. An additional promoter region not carrying an evident
484 match to the FliA consensus, P*hsbA*, showed a similar response pattern to FliA, FleQ and
485 σ^{54}, but the extent of the regulation was moderate in all cases and significant basal
486 transcription was observed in all backgrounds. We propose that this promoter region may
487 contain a weak, previously undetected FliA-dependent promoter and an additional FliA-
488 independent promoter activity.
489

490 **DISCUSSION**

491 The *P. putida* KT2440 flagellar cluster resides in a ~70 kbp chromosomal region
492 encoding the vast majority of structural and regulatory flagellar proteins along with the core
493 components of the chemotaxis machinery. Here we expand on our previous work (Jiménez-
494 Fernández *et al*., 2016; Navarrete *et al*., 2019; Wirebrand *et al*., 2018) to identify the
495 transcriptional organization of the *P. putida* KT2440 flagellar cluster and characterize the
496 transcriptional regulation of twenty primary and internal promoters accounting for the
497 expression of all but three relevant . The results presented provide (i) updated annotations
498 and putative functions for seven flagellar genes; (ii) evidence of the transcriptional
499 organization of the flagellar cluster in ten separate operons, while an additional operon,
500 *motAB*, is not linked to the cluster; (iii) an inventory of twenty-two flagellar promoters,
501 including eleven primary and eleven internal promoters; (iv) characterization of the
502 regulation of all twenty-two flagellar promoters regarding their dependence on known
503 flagellar transcription factors (FleQ, FleR, FliA, σ^{54}), the auxiliary protein FleN and the
504 intracellular signalling molecule c-di-GMP; (v) a novel hierarchy for the transcriptional
505 cascade controlling flagellar gene expression that differs significantly from those previously
506 described; (vi) evidence of high conservation of the flagellar gene complement and
507 organization in the genus *Pseudomonas*; and (vii) evidence of high conservation of the
508 flagellar promoter motifs in a set of environmental *Pseudomonas*, suggesting that many of
509 the results presented here may be applicable to this group of organisms.

510 We have defined the *P. putida* KT2440 flagellar cluster as the chromosomal region
511 encompassing ORFs PP_4328 (*fliK2*) to PP_4397 (*flgZ*). These boundaries were
512 established based on three lines of evidence. (i) High conservation: 51 of the flagellar genes
513 are present in all the *Pseudomonas* genomes analyzed; the remaining 8 are found in at least
514 80%; (ii) conservation of gene arrangement: all flagellar genes are clustered in the same
515 order in one to three chromosomal locations in most *Pseudomonas* genomes analyzed
516 (**Supplementary File 1**); and (iii) experimental evidence of involvement in flagellar function:

517 all but one of the 59 flagellar genes in the cluster have been demonstrated to play roles
518 related to assembly and operation of the flagellar and chemotaxis complexes in at least one
519 organism. In addition to the genes previously annotated, we have been able to identify an
520 ortholog to *H. pylori flhX*, encoding a small protein similar to the processed form of FlhB that
521 determines the specificity switch of the FT3SS (Pallen *et al*., 2005). FlhX has been shown
522 to partially complement FlhB function in *H. pylori* (Smith *et al*., 2009), but its actual role in
523 flagellar assembly is not well understood. One more gene in the cluster is an ortholog of *V.*
524 *cholerae flrD*, encoding a transmembrane signal transduction protein that stimulates
525 transcriptional activation by the FlrBC two-component system (equivalent to FleSR) (Moisi
526 *et al*., 2009). We have also identified orthologs of *Vibrio* spp. *parP* and *parC*, encoding two
527 polar landmark proteins required for polar positioning of the chemotaxis arrays (Ringgaard
528 *et al*., 2018). Finally, we have annotated the orthologs of *P. aeruginosa hptB*, *hsbR* and
529 *hsbA*, encoding a phosphotransferase a response regulator and an anti-σ factor antagonist
530 proteins. This system antagonizes FlgM sequestration of FliA by partner-switching
531 mechanism (Bhuwan *et al*., 2012) and indirectly regulates biofilm formation by regulating
532 the activity of the diguanylate cyclase HsbD (Valentini *et al*., 2016). In contrast, the function
533 of *fliK2* is still uncharacterized. However, because *fliK2* is part of an operon with *flhX*, and
534 its transcription is FliA-dependent in *P. putida*, we find it likely that it will eventually
535 demonstrate to be a *bona fide* flagellar gene. With the updated annotation, we conclude that
536 the conserved *Pseudomonas* flagellar cluster gene set encodes all the structural proteins of
537 the flagellum (minus an additional flagellar motor encoded by the *motAB* operon elsewhere),
538 all the elements required for flagellar assembly (including the complete FT3SS), all the core
539 components of the chemotaxis apparatus, three dedicated transcription factors, seven
540 auxiliary proteins to control their activity, three landmark proteins for the polar location of the
541 flagellar and chemotaxis complexes, and one protein involved in functional regulation of
542 flagellar rotation (**Supplementary Table 1**). We note that, in addition to the conserved gene

543 complement described here, some organisms bear species- or strain-specific flagellar
544 genes in their clusters [e.g., genes for flagellin glycosylation (Dasgupta *et al*., 2003)].

545 The *P. putida* KT2440 flagellar cluster is organized in ten transcriptional units, with
546 primary promoters located upstream from *fliK2*, *flhA*, *hsbA*, *fliH*, *fliE*, *fliC*, *flgF*, *flgB*, *cheV*
547 and *flgA*. In addition, internal promoters are found upstream from *flhF*, *cheA* and *parC* at the
548 *flhAF-fleN-fliA-cheYZAB-motCD-parCP-cheW-flrD* operon, upstream from *fliK* and *fliL* at the
549 *hsbAR-hptB-fliKLMNOPQE-flhB* operon, upstream from *fliD*, *fliS*, *fleQ* and *fleS* at the *fliC-*
550 *flaG-fliDST-fleQRS* operon and upstream from *flgM* and *flgZ* at the *flgAMNZ* operon (**Fig.**
551 **2**). Some of the promoters shown here were identified and partially characterized in our
552 previous work (Jiménez-Fernández *et al*., 2016; Navarrete *et al*., 2019; Wirebrand *et al*.,
553 2018)**.** Our results indicate that much of the *P. putida* KT2440 flagellar cluster is transcribed
554 as part of long operons containing internal promoters. The recent development of high
555 throughput RNA-sequencing techniques with the possibility of genome-wide mapping of
556 transcriptional start and termination sites has revealed that nested operon architectures are
557 much more common in bacterial genomes than expected (Conway *et al*., 2014; Vera *et al*.,
558 2020; Warrier *et al*., 2018; Yan *et al*., 2018).

559 While the operon arrangement described here is generally reminiscent to that
560 proposed for *P. aeruginosa* (Dasgupta *et al*., 2003), the *P. aeruginosa* cluster does not
561 contain any operons with a nested architecture. Rather, the genes are grouped in shorter
562 transcriptional units. We observe that the *P. aeruginosa* counterparts to the internal
563 promoters shown here are regarded as primary promoters, which leads to the division of
564 these operons into shorter transcriptional units. Whether this is the result of interspecies
565 differences within *Pseudomonas* or a consequence of the different approaches used to
566 characterize the transcriptional organization of these genes remains to be determined. It is
567 noteworthy that long, nested flagellar operons have been described in other polarly-
568 flagellated Gamma-proteobacteria (Y. K. Kim and McCarter, 2000; Prouty *et al*., 2001;
569 Wilhelms *et al*., 2011; Wu *et al*., 2011).

570 The regulatory architecture of the flagellar transcriptional cascade has been elucidated
571 in the polarly flagellated Gamma-proteobacteria *V. cholerae* (Prouty *et al*., 2001), *Vibrio*
572 *parahemolyticus* (McCarter, 2001), *Vibrio campbelli* (Petersen *et al*., 2021), *Legionella*
573 *pneumophila* (Albert-Weissenberger *et al*., 2010), *Aeromonas hydrophila* (Wilhelms *et al*.,
574 2011), *Shewanella oneidensis* (Shi *et al*., 2014), *P. aeruginosa* (Dasgupta *et al*., 2003) and
575 now *P. putida* (**Fig. 7**). Comparative analysis of the models proposed in these organisms
576 suggests a number of common themes along with significant organism-to-organism
577 variability even within the same genus. All the transcriptional cascades described are three-
578 or four-tiered, with the transcription factor FleQ (also known as FlrA) at the top of the
579 regulatory hierarchy. Accordingly, *fleQ/flrA* is invariably a Class I gene (i.e., its transcription
580 does not require any of the dedicated flagellar transcription factors). Synthesis of FleQ/FlrA
581 is likely activated in response to environmental and physiological cues that favor a motile
582 lifestyle, but the conditions and regulatory mechanisms involved are generally not well
583 understood. Regulation of *fleQ* expression in diverse *Pseudomonas* species may involve
584 repression by the CRP ortholog Vfr (Dasgupta *et al*., 2002), AmrZ (Tart *et al*., 2006), OsaR
585 (Ma *et al*., 2021) and activation by the AlgU-regulated antisense RNA $fleQ_{as}$ (Markel *et al*.,
586 2018). We have found that P*fleQ* is induced in stationary phase and not regulated by FleQ,
587 FleR or FliA, suggesting that it belongs to Class I (**Fig. 4A**). Since transcription from P*fleQ*
588 is not interrupted at the intergenic region between *fleQ* and *fleS* (**Fig. 2E and F**), *fleQ*, *fleS*
589 and *fleR* must be considered Class I flagellar genes in *P. putida*, even though *fleS* and *fleR*
590 are also transcribed from their own FleQ-dependent promoter. Although we have not
591 explored regulation of the P*fleQ* promoter further, we note that the AlgU-dependent promoter
592 motifs for $fleQ_{as}$ are conserved in a wide range of *Pseudomonas* (Markel *et al*., 2018), and
593 we observe significant levels of antisense transcription around the 5' end of *fleQ* coding
594 sequence (**Fig. 2E**), suggesting that $fleQ_{as}$ may also be produced and operate in *P. putida*.
595 A second promoter, P*fliH* driving the synthesis of the secretion ATPase components FliH,
596 FliI and FliJ, showed a similar behavior to P*fleQ*: its expression was low in exponential

597 phase, induced in stationary phase and unresponsive to any of the dedicated flagellar
598 transcriptions factors (**Fig. 4B**). Accordingly, we also classify FliH, FliI and FliJ as Class I
599 genes. We note that the presence of additional Class I genes other than the master
600 regulation is not uncommon in polarly flagellated Gamma-proteobacteria (Dasgupta *et al*.,
601 2003; Petersen *et al*., 2021; Wilhelms *et al*., 2011), and *flrB* and *flrC* are actually Class I
602 genes in *V. campbellii* (Petersen *et al*., 2021).

603 FleQ activation of Class II genes sets in motion the assembly of the basal body (**Fig.**
604 **7**). Polar localization of the flagella is directed by the signal recognition particle-like GTPase
605 FlhF (Schuhmacher *et al*., 2015). FlhF is likely the first flagellar gene product to locate to the
606 cell pole and has been shown to recruit the first assembly building block, the MS-ring
607 structural protein FliF, in *V. cholerae* (Green *et al*., 2009). As basal body assembly
608 progresses, the MinD-like ATPase FleN (also known as FlhG) provides a negative regulatory
609 loop by inhibiting the ATPase activity of FleQ, required for σ^{54} promoter activation (**Fig. 7**)
610 (Baraquet and Harwood, 2013). Deletion of *fleN* provokes hyperflagellation and *fleN*
611 overexpression prevents the synthesis of flagella (Schuhmacher, *et al*., 2015), suggesting
612 that it may become active in response to an checkpoint that indicates that assembly of the
613 correct number of flagella has been initiated. Recently, Blagotinsek *et al*., (2020) showed
614 that FlhG is recruited to the flagellar pole as an inactive monomer by the C-ring protein FliM
615 in *S. oneidensis*. Membrane-bound FlhG may then undergo ATP-induced dimerization to
616 become active in a process that is stimulated by interaction with membrane lipids
617 (Schuhmacher *et al*., 2015). The ATP-bound dimer is the form that interacts with FleQ to
618 prevent Class II promoter activation (Baraquet and Harwood, 2013). Thus, assembly of the
619 C-ring(s) may be the signal that triggers FleN-dependent inhibition of Class II promoter
620 transcription. The extent of flagellar assembly enabled by FleQ-activated transcription is
621 most often restricted to all or part of the early basal body (EBB) structures, namely the MS-
622 ring, the C-ring and the FT3SS (Dasgupta *et al*., 2003; Khan *et al*., 2020). In contrast, we
623 have shown that *P. putida* Class II genes encode all structural flagellar components except

624 for the filament. This arrangement is reminiscent of that proposed for *V. campbellii* (Petersen
625 *et al*., 2021) and *S. oneidensis* (Shi *et al*., 2014).

626 An additional tier, Class III, activated by the FleSR (also known as FlrBC) two-
627 component system is required in *P. aeruginosa*, *V. cholerae*, *V. parahemolyticus* and *A.*
628 *hydrolitica* to complete the assembly of the components of the hook-basal body (HBB)
629 complex (Dasgupta *et al*., 2003; Khan *et al*., 2020; Wilhelms *et al*., 2011). Activation of
630 FleSR/FlrBC was recently shown to respond to the assembly of the EBB in *V. cholerae* and
631 *P. aeruginosa* (Burnham *et al*., 2020), as previously observed with the Epsilon-
632 proteobacteria *Campylobacter jejuni* and *Helicobacter pylori* (Boll and Hendrixson, 2013;
633 Tsang and Hoover, 2015). Sensing of the assembly status may be mediated by FlrD, a
634 membrane protein containing a HAMP domain that stimulates FlrBC-dependent activation
635 in *V. cholerae* (Moisi *et al*., 2009)**.** *P. putida* encodes orthologs of FlrD and FleSR
636 (**Supplementary Table S1**). However, because transcription of all the HBB genes is directly
637 dependent on FleQ, FleR is not essential for the assembly of functional flagella
638 (**Supplementary Fig. S6**). Yet, we have shown that FleR shows statistically significant
639 effects on the transcription of multiple flagellar promoters. Particularly, transcription from the
640 P*flgB* and P*flgF* promoters, driving the synthesis of the structural rod, LP ring and hook
641 proteins, is somewhat diminished in the Δ*fleR* strain (**Fig. 5**), and sequence alignment
642 revealed multiple conserved sequences with high similarity to the proposed FlrC binding
643 motif (CGGCAA) in our set of seven environmental *Pseudomonas* strains in both promoter
644 regions (**Supplementary File 2**). These observations suggest that FleR may play an
645 unrecognized role in the synthesis of the late basal body and hook components.
646 Interestingly, replacement of the *V. cholerae* P*flgB*, P*flgF* and P*flgK* FlrC-dependent
647 promoters for the FlrA-dependent P*fliE* resulted in normal flagellation and motility in the wild-
648 type strain, but provoked the loss of the flagellum and motility in a Δ*flhG* background,
649 suggesting that the FlrBC may provide robustness to the regulatory circuit in the event of
650 faulty FlhG function (Burnham *et al*., 2020). Accordingly, we hypothesize that FleSR

651 activation of the P*flgB* and P*flgF* promoters in *P. putida* may act as a safeguard against a
652 shortage of rod and hook subunits if FleQ activation is compromised by altered FleN
653 signaling. While this evidently does not happen in our experimental setting, there may be
654 conditions in which such backup activation by FleR may relevant. Overlapping functions of
655 FleQ and FleR have been documented in a few other systems. FlrC, the FleR ortholog of *S.*
656 *oneidensis*, is not required for motility and plays a minor role in the regulation of the flagellar
657 promoters (Shi *et al*., 2014). In this organism ectopic production of FlrC can suppress the
658 nonmotile phenotype of a Δ*flrA* mutant (lacking the cognate FleQ ortholog) by replacing FlrA
659 as the activator of the flagellar σ^{54}-dependent promoters (Gao *et al*., 2018). In a similar vein,
660 the functions of FlrA and FlrC are partially redundant in the flagellar cascade of *V. campbelli*;
661 however, in this case, it is FlrA, and not FlrC, that is dispensable for flagellar motility
662 (Petersen *et al*., 2021). Finally, in *Rhodobacter sphaeroides*, FleQ and the FleR ortholog
663 FleT cooperate in the regulation of Class III flagellar promoters by forming a
664 heterooligomeric protein (Poggio *et al*., 2005). These and other possibilities of interplay
665 between the two *P. putida* σ^{54}-dependent activators are worth exploring in the future.

666 The final tier in the flagellar cascades is triggered by the release of FliA from
667 inactivation by the anti-σ factor FlgM. As first demonstrated in *Salmonella*, a shift in secretion
668 specificity upon completion of the hook structure leads to FlgM secretion by way of the
669 FT3SS (Karlinsey *et al*., 2000). This is generally considered to be a conserved mechanism
670 to activate FliA-dependent transcription in an assembly checkpoint-dependent fashion, and
671 has been directly demonstrated in *V. cholerae* (Correa *et al*., 2004). In addition, the *P.*
672 *aeruginosa* anti-sigma factor antagonist HsbA has been show to prevent FlgM-dependent
673 inactivation of FliA by a partner-switching mechanism in response to a phosphorylation
674 cascade involving several membrane hybrid sensor kinases, the histidine
675 phosphotransferase HtpB and the response regulator HsbR (Bhuwan *et al*., 2012), but the
676 signals triggering this system are currently not known and its connection with flagellar

677 assembly is therefore unclear. As the *P. putida* flagellar cluster encodes FlgM, HsbA, HsbR
678 and HtpB orthologs (**Supplementary Table S1**), any of these mechanisms may be
679 functional, but we have not explored them in this work. The set of FliA-dependent Class IV
680 genes in polarly flagellated Gamma-proteobacteria normally includes flagellin and other
681 filament components, along with chemotaxis and flagellar stator genes. In *P. putida* FliA is
682 essential for expression of *fliC* and *flaG*, encoding flagellin and a regulator of filament length,
683 the chemotaxis operon *cheVR*, the stator genes *motAB* and the uncharacterized *fliK2-flhX*
684 operon (**Figs. 2, 5, 6 and 7**), and boosts transcription of the distal chemotaxis and stator
685 genes of the Class II *flhAF-fleN-fliA-cheYZAB-motCD-parCP-cheW-flrD* operon.
686 Accordingly, FliA is essential for assembly of the filament and completion of the chemotaxis
687 signal transduction system and one of the stator complexes (**Fig. 7**). We note that, although
688 the core chemotaxis and the *motCD* stator genes were previously assigned to Class IV in
689 *P. aeruginosa* (Dasgupta *et al*., 2003), re-examination of the evidence revealed that none of
690 the orthologs of the *flhAF-fleN-fliAcheYZAB-motCD-parCP-cheW-flrD* operon genes were
691 significantly downregulated in a Δ*fliA* mutant, and should therefore be re-classified as Class
692 II [(see Supplementary Tables 2-6 in Dasgupta *et al*. (2003)]

693 FliA also participates in feed-forward and feedback loops on several regulatory
694 elements (**Fig. 7)**. On the one hand, it boosts the synthesis of the anti-sigma FlgM (**Fig. 6**),
695 an antagonist of FliA itself. Most intriguingly, FliA-dependent transcription of *fleQ* and *fleSR*
696 as part of the *fliC-flaG-fliDST-fleQSR* operon (**Fig. 2**) provides positive feedback to the
697 synthesis of the transcription factors involved in early flagellar gene expression (**Fig. 7**).
698 Since FleQ function and Class II transcription may be transiently impaired by the formation
699 of an inactive complex with FleN (Baraquet and Harwood, 2013), FleQ newly synthesized
700 by way of readthrough transcription from the strong Class III P*fliC* promoter may titrate out
701 FleN, restoring expression of the Class II genes. Unlike peritrichous flagellates, in which
702 new flagella can be continuously added during cell elongation, polar flagellates such as *P.*
703 *putida* must assemble their flagella in a discontinuous fashion, as a new pole is generated

704 only once per cell cycle during cell division. New flagella must then be assembled at the new
705 pole in time for their completion at the following cell division. In this scenario, the reactivation
706 of early flagellar gene expression by this FliA-mediated positive feedback mechanism
707 appears to be a suitable mechanism to enable *de novo* flagella synthesis at the new pole
708 while assembly at the old pole is completed.
709

710 **EXPERIMENTAL PROCEDURES**

711 **Bacterial strains and growth conditions**

712 The bacterial strains used in this work are summarized in **Supplementary Table S4.**
713 Liquid cultures of *E. coli* and *P. putida* strains were routinely grown in Luria-Bertani (LB)
714 broth (Sambrook and Russell, 2000) at 37°C and 30 °C, respectively, with 180 rpm shaking.
715 For fluorescence monitoring, 1/10 strength LB was used to minimize background
716 fluorescence. For solid media, Bacto-Agar (Difco) was added to a final concentration of 18
717 g l^{-1}. Antibiotics and other additions were used, when required, at the following
718 concentrations: ampicillin (100 mg l^{-1}), carbenicillin (0.5 g l^{-1}), kanamycin (25 mg l^{-1}),
719 rifampicin (10 mg l^{-1}), chloramphenicol (15 mg l^{-1}), gentamycin (10 mg l^{-1}), tetracycline (5
720 mg l^{-1}), 5-bromo-4-chloro-3-indoyl-β-D-galactopyranoside (X-gal) (25 mg l^{-1}) and sodium
721 salicylate (from 0.1 mM to 2 mM) All reagents were purchased from Sigma Aldrich, except
722 for X- Gal, which was purchased from Fermentas.

723 **Plasmid and strain construction**

724 Plasmids and oligonucleotides used in this work are summarized in **Supplementary**
725 **Table S4.** All DNA manipulations were performed following standard procedures (Sambrook
726 and Russell, 2000). Restriction and modification enzymes were used according to the
727 manufacturers' instructions (Fermentas, Roche and NEB) When required, blunt ends were
728 generated using the Klenow fragment or T4 DNA polymerase. *E. coli* DH5α was used as a
729 host in cloning procedures. All cloning steps involving PCR were verified by commercial
730 sequencing (Secugen or Stab Vida) Plasmid DNA was transferred to *E. coli* and *P. putida*
731 strains by transformation (Inoue *et al*., 1990), triparental mating (Espinosa-Urgel *et al*., 2000)
732 or electroporation (Choi *et al*., 2006). Site-specific integration of miniTn7 derivatives in *P.*
733 *putida* strains was performed essentially as described (Choi *et al*., 2005). The flagellar
734 cluster and *rpoN* gene were deleted by plasmid-based gene replacement as previously
735 described (Martínez-García and de Lorenzo, 2021). For *rpoN* deletion, 500-bp fragments
736 flanking the respective gene were PCR-amplified with oligonucleotide pairs rpoN-fwd-

737 EcoRI/rpoN-overlap-Rev (upstream region) and rpoN-overlap-fwd/rpoN-rev-BamHI
738 (downstream region), subsequently combined by overlap extension PCR and cloned via
739 *Eco*RI and *Bam*HI restriction sites into plasmid pEMG, a Km-resistant plasmid that
740 incorporates two I-SceI sites flanking a *lacZ*α polylinker, to yield pMRB290. For flagellar
741 cluster deletion, the plasmid pEMG-flagella (Martínez-García *et al*., 2014) containing 750-
742 bp upstream and 816-bp downstream of PP_4297 and PP_4329 genes respectively was
743 used. These plasmids were mobilised by triparental mating to *P. putida* KT2442 harbouring
744 the I-SceI expressing plasmid pSW-I (Martínez-García and de Lorenzo, 2011) The positive
745 co-integrates were selected through PCR amplification of flanking regions and resolved
746 through induction of the I-SceI enzyme, derived from the pSW-I plasmid using 15 mM 3-
747 methyl benzoate (3-MB) Then, the induced culture was plated onto LB agar plates and the
748 positive colonies were assessed for the loss of the Km resistance marker. Deletions were
749 verified by PCR. The pSW-I plasmid was cured after successive passes of the deleted
750 strains in LB without antibiotics.
751 To construct *P. putida* KT2442 derivatives with in-frame deletions of *fleN*, *fleQ* and *fleR*,
752 upstream and downstream chromosomal regions flanking these genes were PCR-amplified
753 with an specific oligonucleotide pairs. For *fleN* deletion, fleN-up-fwd/fleN-up-rev (upstream
754 region) and fleN-down-fwd/fleN-down-rev (downstream region) For *fleQ* deletion, fleQ-up-
755 fwd/fleQ-up-rev (upstream region) and fleQ-down-fwd/fleQ-down-rev (downstream region)
756 For *fleR* deletion, fleR-up-fwd-EcoRI/fleR-up-rev-BamHI (upstream region) and fleR-down-
757 fwd-BamHI/fleR-down-rev-HindIII (downstream region) The PCR products were cleaved
758 with EcoRI and BamHI or BamHI and HindIII, respectively, and three-way ligated into EcoRI-
759 and HindIII- digested pEX18Tc, a gene replacement vector. A BamHI-excised FRT-flanked
760 kanamycin resistance cassette from pMPO284 was then cloned into the BamHI site, yielding
761 pMRB96 (*fleQ*), pMRB104 (*fleN*) and pMRB192 (*fleR*) These plasmids were transferred to
762 *P. putida* KT2442 by electroporation. Selection of integration, allelic replacement and FLP-
763 mediated excision of the kanamycin resistance marker was performed essentially as

764 described (Hoang *et al*., 1998; Llamas *et al*., 2000) to generate Δ*fleQ* (MRB52), Δ*fleN*
765 (MRB71) and Δ*fleR* (MRB93) The structure of the deleted loci was verified by PCR.

766 For the construction of pMRB178 and pMRB286, plasmids producing FleQ and FliA,
767 respectively, the *fleQ* and *fliA* open reading frames were PCR-amplified with the
768 oligonucleotide pairs FleQ-XbaI-SD-fwd/ FleQ-SpeI-rev and FliA-fwd-XbaI-SD/FliA-rev-
769 SpeI-Stop, digested with appropriated enzymes and cloned into XbaI- and SpeI-cleaved
770 pMRB172, a salicylate-inducible expression plasmid bearing Tn7 transposon for site-
771 specific genome integration.

772 A 750-bp fragment containing the putative P*fleS* promoter region (positions -750 to -
773 1 relative to *fleS* start codon) was amplified using oligonucleotides PfleS-fwd/PfleS-rev as
774 primers and cloned via SpeI and PstI restriction sites into previously cleaved pMRB196, a
775 pMRB3-derived broad host-range *gfp*mut3::*lac*Z transcriptional fusion vector, yielding
776 pMRB291. P*fliE* and P*flgF* 500-bp promoter regions were amplified by using oligonucleotide
777 pairs PfliE-fwd-SpeI/PfliE-rev-PstI and PflgF-fwd-SpeI/PflgF-rev-PstI and cloned as
778 described above to yield pMRB250 (P*flgF*) and pMRB259 (P*fliE*)

779 **Flagellar motility (swimming) assays**

780 Swimming assays were adapted from Parkinson (1976). Tryptone motility plates
781 containing 0.3% Bacto-agar (Difco) were toothpick-inoculated with fresh colonies and
782 incubated for 14 h at 30°C. At least 3 biological replicates were assayed for each strain.

783 ***In vivo* gene expression assays**

784 Differential rates of GFP accumulation during exponential growth were used to
785 measure gene expression in cultures bearing *gfp-lac*Z transcriptional fusions to different
786 promoters. Overnight LB cultures with the corresponding antibiotics of the fusion-bearing
787 strains were diluted in 1/10 strength LB broth with the same additions, and dispensed into
788 the wells of a Costar 96 microtiter polystyrene plate (Corning) (150 µl per well). The plate
789 was incubated in a Tecan Spark microliter plate reader/incubator at 30 °C with 510 rpm
790 shaking to mid-exponential phase. Cultures were then diluted in the same medium and

791 incubated in the same conditions for 23 hours. A_{600} and GFP fluorescence (485 nm
792 excitation, 535 nm emission) were monitored in 15-minutes intervals during incubation with
793 the gain value set to 55. Differential rates of GFP fluorescence accumulation were calculated
794 as the slopes of the linear regression (R^2>0.98) performed on the exponential growth
795 fluorescence vs. absorbance plots (Supplementary Fig. 3) (Jacob and Monod, 1961). The
796 results (arbitrary units) were divided by 1000 to avoid excessive trailing zeros in the chart
797 axis legends.

798 For end-point fluorescence assays cells bearing the corresponding fusion plasmids
799 grown on LB with the appropriate additions were diluted in 3 ml of the same medium to an
800 A_{600} of 0.01 and incubated at 30°C with shaking (180 rpm) for 24 hours (stationary phase).
801 0.5 ml samples were withdrawn, cells were washed three times in 1xNaCl-phosphate buffer
802 (M9 salts lacking NH_4Cl) (Sambrook and Russell, 2000) suspended in 5 ml 1xNaCl-
803 phosphate buffer. Samples (150 µl) were transferred to Costar 96 plates and end-point
804 absorbance and fluorescence measurements were performed as above.

805 For β-galactosidase assays, the fusion strains were grown and diluted as above and
806 incubated for 4.5 or 24 hours (for exponential or stationary phase assays, respectively).
807 Growth was then stopped, and β-galactosidase activity was determined from sodium
808 dodecyl sulphate- and chloroform-permeabilized cells as described (Miller, 1993). Results
809 are reported as Miller units (Miller, 1993).

810 For all expression assays, data are reported as the average and standard deviation
811 of at least three biological replicates. Significance of the differences reported was assessed
812 by means of the Student's t-test for unpaired samples not assuming equal variance.
813 Differences were considered significant when the *p*-value was below 0.05.

814 **RNA isolation and RT-PCR**

815 Total RNA from stationary phase cultures was extracted as described (García-
816 González *et al*., 2005) Reverse transcription (RT) of total RNA (2 µg) was carried out using
817 the High-Capacity cDNA Achieve kit (Applied Biosystems) following the manufacturer

818 instructions. Amplification reactions were performed with 50 ng of cDNA as template in a
819 30-cycle PCR program, using appropriate oligonucleotides detailed in **Supplementary**
820 **Table S2** and Illustra™ PuReTaq™ Ready-To-Go™ PCR Beads (GE Healthcare) Negative
821 and positive controls were performed with total RNA or genomic DNA as templates,
822 respectively. The RT-PCR products obtained were resolved by 1% agarose gel
823 electrophoresis and visualized by ethidium bromide staining.

824 **RNA-seq assay**

825 5 µg of total RNA were sent to the CABIMER Genomics facility (Seville, Spain)
826 Depletion of rRNA and preparation of cDNA libraries were carried out with the Illumina
827 Stranded TOTAL RNA preparation RIBO-ZERO PLUS kit. Single-end sequencing was
828 performed with the Illumina NextSeq 500 HIGH-Output flow cell and 1 x75 bp length
829 parameters at the CABIMER Genomics unit (Centro Andaluz de Biología molecular y
830 Medicina regenerativa, Sevilla, Spain)..

831 The RNA-seq raw data was pre-filtered using FASTQ Toolkit v.1.0.0. Quality of the
832 reads was checked with FastQC
833 (https://www.bioinformatics.babraham.ac.uk/projects/fastqc/) and then mapped to the *P.*
834 *putida* KT2440 reference genome (GenBank: NC_002947.4) using Bowtie2 v.2.3.5.1
835 (Langmead and Salzberg (2012). Mapped data were converted to BAM files using Samtools
836 v1.11 (Li *et al*., 2009) and reads were visualized with the Integrative Genomics Viewer (IGV)
837 (Robinson *et al*., 2011). Raw dataset is available at the Gene Expression Omnibus (GEO)
838 database (http://www.ncbi.nlm.nih.gov/geo) under accession number GEO: GSE173832.
839 The genome-aligned data were displayed using the Integrated Genomics Viewer (IGV)
840 software.

841 **Bioinformatics methods**

842 We used the pre-computed *Pseudomonas* ortholog groups available at the
843 *Pseudomonas* genome database (Winsor *et al*., 2016) (pseudomonas.com) to assess the
844 conservation of the flagellar gene set in the genus *Pseudomonas*. Synteny was analyzed by

845 computing the number of intervening genes between the orthologs of all consecutive genes
846 in the *P. putida* flagellar cluster in all 550 genomes in the *Pseudomonas* ortholog database
847 using a simple Microsoft Excel script and the numerical part of the Locus Tag for each pair
848 of genes in each genome as a positional reference. The resulting dataset was manually
849 curated and genomes yielding inconsistent or ambiguous results were discarded. A total of
850 401 genomes provided consistent results for the complete cluster (**Supplementary File 1**)
851 Sequence alignment of intergenic sequences used 500 bp fragments upstream from the
852 start codon for each gene. Occasional inconsistencies in the annotation of the start codons
853 were corrected when required. Multiple sequence alignments were performed using
854 MUSCLE (Edgar, 2004), available at https://www.ebi.ac.uk/Tools/msa/muscle/.
855

ACKNOWLEDGMENTS

We wish to thank María G. Velasco, Laura Claret and Álvaro Escobar for their help in some of the constructions used in this work, the CABIMER Genomics unit for their technical help with the RNA-seq assays, Guadalupe Martín for technical assistance and all members of the Govantes and Santero laboratories at CABD and the Andalusian Network of Bacterial Flagella Researchers (RedFlag) for providing materials and critical discussions. This work was funded by the Spanish Ministerio de Ciencia, Innovación y Universidades and European Regional Development fund, grants BIO2013-420173-P and PGC2018-097151-B-I00 awarded to FG. M P-S is the recipient of a PhD training grant (FPU) of the Spanish Ministerio de Ciencia, Innovación y Universidades. The authors declare no conflict of interest.

867 **REFERENCES**

868 Albert-Weissenberger, C., Sahr, T., Sismeiro, O., Hacker, J., Heuner, K., and Buchrieser,
869 C. (2010) Control of flagellar gene regulation in *Legionella pneumophila* and its relation to
870 growth phase. J Bacteriol 192: 446–455. https://doi.org/10.1128/JB.00610-09

871 Altegoer, F., Schuhmacher, J., Pausch, P., and Bange, G. (2014) From molecular evolution
872 to biobricks and synthetic modules: A lesson by the bacterial flagellum. Biotechnol Genet
873 Engin Rev 30: 49–64. https://doi.org/10.1080/02648725.2014.921500

874 Aranda-Olmedo, I., Tobes, R., Manzanera, M., Ramos, J.L., and Marqués, S. (2002)
875 Species-specific repetitive extragenic palindromic (REP) sequences in *Pseudomonas*
876 *putida*. Nucleic Acids Res 30: 1826–1833. https://doi.org/10.1093/nar/30.8.1826

877 Baraquet, C., and Harwood, C. S. (2013) Cyclic diguanosine monophosphate represses
878 bacterial flagella synthesis by interacting with the Walker a motif of the enhancer-binding
879 protein FleQ. Proc Natl Acad Sci USA 110(46), 18478–18483.
880 https://doi.org/10.1073/pnas.1318972110

881 Baraquet, C., Murakami, K., Parsek, M.R., and Harwood, C.S. (2012) The FleQ protein from
882 *Pseudomonas aeruginosa* functions as both a repressor and an activator to control gene
883 expression from the Pel operon promoter in response to c-di-GMP. Nucleic Acids Res 40:
884 7207–7218. https://doi.org/10.1093/nar/gks384

885 Barrios, H., Valderrama, B., and Morett, E. (1999) Compilation and analysis of σ^{54}-
886 dependent promoter sequences. Nucleic Acids Res 27: 4305–4313.
887 https://doi.org/10.1093/nar/27.22.4305

888 Bhuwan, M., Lees, H.J., Pengs, H.L., and Chang, H.Y. (2012) Histidine-containing
889 phosphotransfer protein-B (HptB) regulates swarming motility through partner-switching
890 system in *Pseudomonas aeruginosa* PAO1 strain. J Biol Chem 287: 1903–1914.
891 https://doi.org/10.1074/jbc.M111.256586

892 Blagotinsek, V., Schwan, M., Steinchen, W., Mrusek, D., Hook, J. C., Rossmann, F.,
893 Freibert, S.A., Kratzat, H., Murat, G., Kressler, D., Beckmann, R., Beeby, M., Thormann,
894 K.M., and Bange, G. (2020) An ATP-dependent partner switch links flagellar C-ring
895 assembly with gene expression. Proc Natl Acad Sci USA 117: 20826–20835.
896 https://doi.org/10.1073/pnas.2006470117

897 Blanco-Romero, E., Redondo-Nieto, M., Martínez-Granero, F., Garrido-Sanz, D., Ramos-
898 González, M.I., Martín, M., and Rivilla, R. (2018) Genome-wide analysis of the FleQ direct
899 regulon in *Pseudomonas fluorescens* F113 and *Pseudomonas putida* KT2440. Sci Rep 8:
900 13145. https://doi.org/10.1038/s41598-018-31371-z

901 Boll, J. M., and Hendrixson, D. R. (2013) A regulatory checkpoint during flagellar biogenesis
902 in *Campylobacter jejuni* initiates signal transduction to activate transcription of flagellar
903 genes. MBio 4: e00432-13. https://doi.org/10.1128/mBio.00432-13

904 Bouteiller, M., Dupont, C., Bourigault, Y., Latour, X., Barbey, C., Konto-ghiorghi, Y., and
905 Merieau, A. (2021) *Pseudomonas* flagella: Generalities and specificities. Int J Mol Sci 22:
906 3337. https://doi.org/10.3390/ijms22073337

907 Bown, J.A., Barne, K.A., Minchin, S.D., and Busby, S.J.W. (1997) Extended -10 promoters.
908 In Mechanisms of transcription. Eckstein, F., and Lilley, D. M. J. (eds) Berlin-Heidelberg:
909 Springer, pp. 41–52. https://doi.org/10.1007/978-3-642-60691-5_4

910 Burnham, P.M., Kolar, W.P., and Hendrixson, D.R. (2020) A polar flagellar transcriptional
911 program mediated by diverse two-component signal transduction systems and basal
912 flagellar proteins is broadly conserved in polar flagellates. MBio 11: e03107-19
913 https://doi.org/10.1128/mBio.03107-19

914 Chevance, F.F.V., and Hughes, K.T. (2008) Coordinating assembly of a bacterial
915 macromolecular machine. Nat Rev Microbiol 6: 455–465.
916 https://doi.org/10.1038/nrmicro1887

917 Choi, K.H., Gaynor, J.B., White, K.G., Lopez, C., Bosio, C.M., Karkhoff-Schweizer, R.A.R.,
918 and Schweizer, H. P. (2005) A Tn7-based broad-range bacterial cloning and expression
919 system. Nat Meth 2: 443–448. https://doi.org/10.1038/nmeth765

920 Choi, K.H., Kumar, A., and Schweizer, H. P. (2006) A 10-min method for preparation of
921 highly electrocompetent *Pseudomonas aeruginosa* cells: Application for DNA fragment
922 transfer between chromosomes and plasmid transformation. J Microbiol Methods 64: 391–
923 397. https://doi.org/10.1016/j.mimet.2005.06.001

924 Conway, T., Creecy, J.P., Maddox, S.M., Grissom, J.E., Conkle, T.L., Shadid, T.M., *et al*.
925 (2014) Unprecedented high-resolution view of bacterial operon architecture revealed by
926 RNA sequencing. MBio 5: e01442-14. https://doi.org/10.1128/mBio.01442-14

927 Corral-Lugo, A., De la Torre, J., Matilla, M.A., Fernández, M., Morel, B., Espinosa-Urgel, M.,
928 and Krell, T. (2016) Assessment of the contribution of chemoreceptor-based signalling to
929 biofilm formation. Environ Microbiol 18: 3355–3372. https://doi.org/10.1111/1462-
930 2920.13170

931 Correa, N.E., Barker, J.R., and Klose, K.E. (2004) The *Vibrio cholerae* FlgM homologue is
932 an anti-σ^{28} factor that is secreted through the sheathed polar flagellum. J Bacteriol 186:
933 4613–4619. https://doi.org/10.1128/JB.186.14.4613-4619.2004

934 Dasgupta, N., Arora, S.K., and Ramphal, R. (2000) *fleN*, a gene that regulates flagellar
935 number in *Pseudomonas aeruginosa*. J Bacteriol 182:, 357–364.
936 https://doi.org/10.1128/JB.182.2.357-364.2000

937 Dasgupta, N., Ferrell, E.P., Kanack, K.J., West, S.E. H., and Ramphal, R. (2002) *fleQ*, the
938 gene encoding the major flagellar regulator of *Pseudomonas aeruginosa*, is σ^{70} dependent
939 and is downregulated by Vfr, a homolog of *Escherichia coli* cyclic AMP receptor protein. J
940 Bacteriol 184: 5240–5250. https://doi.org/10.1128/JB.184.19.5240-5250.2002

941 Dasgupta, N., and Ramphal, R. (2001) Interaction of the antiactivator FleN with the

942 transcriptional activator FleQ regulates flagellar number in *Pseudomonas aeruginosa*. J
943 Bacteriol 183: 6636–6644. https://doi.org/10.1128/JB.183.22.6636-6644.2001

944 Dasgupta, N., Wolfgang, M.C., Goodman, A.L., Arora, S.K., Jyot, J., Lory, S., and Ramphal,
945 R. (2003) A four-tiered transcriptional regulatory circuit controls flagellar biogenesis in
946 *Pseudomonas aeruginosa*. Mol Microbiol 50: 809–824. https://doi.org/10.1046/j.1365-
947 2958.2003.03740.x

948 Echazarreta, M.A., and Klose, K.E. (2019) *Vibrio* flagellar synthesis. Front Cell Infect
949 Microbiol 9: 131. https://doi.org/10.3389/fcimb.2019.00131

950 Edgar, R.C. (2004) MUSCLE: A multiple sequence alignment method with reduced time and
951 space complexity. BMC Bioinformatics 5: 13. https://doi.org/10.1186/1471-2105-5-113

952 Espinosa-Urgel, M., Salido, A., and Ramos, J.L. (2000) Genetic analysis of functions
953 involved in adhesion of *Pseudomonas putida* to seeds. J Bacteriol 182: 2363–2369.
954 https://doi.org/10.1128/JB.182.9.2363-2369.2000

955 Evans, L.D.B., Hughes, C., and Fraser, G.M. (2014) Building a flagellum outside the
956 bacterial cell. Trends Microbiol 22: 566-572. https://doi.org/10.1016/j.tim.2014.05.009

957 Frisk, A., Jyot, J., Arora, S.K., and Ramphal, R. (2002) Identification and functional
958 characterization of *flgM*, a gene encoding the anti-sigma 28 factor in *Pseudomonas*
959 *aeruginosa*. J Bacteriol 184: 1514–1521. https://doi.org/10.1128/JB.184.6.1514-1521.2002

960 Gao, T., Shi, M., and Gao, H. (2018) Partially reciprocal replacement of FlrA and FlrC in
961 regulation of *Shewanella oneidensis* flagellar biosynthesis. J Bacteriol 200: e00796-17
962 https://doi.org/10.1128/JB.00796-17

963 García-Fontana, C., Reyes-Darias, J.A., Muñoz-Martínez, F., Alfonso, C., Morel, B., Ramos,
964 J.L., and Krell, T. (2013) High specificity in CheR methyltransferase function: CheR2 of
965 *Pseudomonas putida* is essential for chemotaxis, whereas CheR1 is involved in biofilm
966 formation. J Biol Chem 288: 18987–18999. https://doi.org/10.1074/jbc.M113.472605

967 García-González, V., Govantes, F., Porrúa, O., and Santero, E. (2005) Regulation of the
968 *Pseudomonas* sp. strain ADP cyanuric acid degradation operon. L Bacteriol 187: 155-167.
969 https://doi.org/10.1128/JB.187.1.155-167.2005.

970 Green, J.C.D., Kahramanoglou, C., Rahman, A., Pender, A.M.C., Charbonnel, N., and
971 Fraser, G.M. (2009) Recruitment of the earliest component of the bacterial flagellum to the
972 old cell division pole by a membrane-associated Signal Recognition Particle family GTP-
973 binding protein. J Mol Biol 391: 679–690. https://doi.org/10.1016/j.jmb.2009.05.075

974 Gross, R., Hauer, B., Otto, K., and Schmid, A. (2007) Microbial biofilms: New catalysts for
975 maximizing productivity of long-term biotransformations. Biotechnol Bioeng 98: 1123–1134.
976 https://doi.org/10.1002/bit.21547

977 Harwood, C.S., Fosnaugh,K., and Dispensa, M. (1989) Flagellation of *Pseudomonas putida*
978 and analysis of its motile behavior. J Bacteriol 171: 4063–4066.
979 https://doi.org/10.1128/jb.171.7.4063-4066.1989

980 Hickman, J.W., and Harwood, C.S. (2008) Identification of FleQ from *Pseudomonas*
981 *aeruginosa* as a c-di-GMP-responsive transcription factor. Mol Microbiol 69: 376–389.
982 https://doi.org/10.1111/j.1365-2958.2008.06281.x

983 Hoang, T.T., Karkhoff-Schweizer, R.R., Kutchma, A.J., and Schweizer, H.P. (1998) A broad-
984 host-range Flp-FRT recombination system for site-specific excision of chromosomally-
985 located DNA sequences: Application for isolation of unmarked *Pseudomonas aeruginosa*
986 mutants. Gene 212: 77–86. https://doi.org/10.1016/S0378-1119(98)00130-9

987 Inoue, H., Nojima, H., and Okayama, H. (1990) High efficiency transformation of *Escherichia*
988 *coli* with plasmids. Gene 96: 23–28. https://doi.org/10.1016/0378-1119(90)90336-P

989 Jacob, F., and Monod, J. (1961) Genetic regulatory mechanisms in the synthesis of proteins.
990 J Mol Biol 3: 318–356. https://doi.org/10.1016/S0022-2836(61)80072-7

991 Jiménez-Fernández, A., López-Sánchez, A., Jiménez-Díaz, L., Navarrete, B., Calero, P.,

992 Platero, A.I., and Govantes, F. (2016) Complex Interplay between FleQ, cyclic diguanylate
993 and multiple σ factors coordinately regulates flagellar motility and biofilm development in
994 *Pseudomonas putida*. PLoS One 11: 1–26. https://doi.org/10.1371/journal.pone.0163142

995 Karlinsey, J.E., Tanaka, S., Bettenworth, V., Yamaguchi, S., Boos, W., Aizawa, S. I., and
996 Hughes, K.T. (2000) Completion of the hook-basal body complex of the *Salmonella*
997 *typhimurium* flagellum is coupled to FlgM secretion and fliC transcription. Mol Microbiol 37:
998 1220-1231. https://doi.org/10.1046/j.1365-2958.2000.02081.x

999 Kearns, D.B. (2010) A field guide to bacterial swarming motility. Nat Rev Microbiol 8: 634–
1000 644. https://doi.org/10.1038/nrmicro2405

1001 Khan, F., Tabassum, N., Anand, R., and Kim, Y.M. (2020) Motility of *Vibrio* spp.: regulation
1002 and controlling strategies. Appl Microbiol Biotechnol 104: 8187–8208.
1003 https://doi.org/10.1007/s00253-020-10794-7

1004 Kim, J.S., Kim, Y.H., Anderson, A.J., and Kim, Y.C. (2014) The sensor kinase GacS
1005 negatively regulates flagellar formation and motility in a biocontrol bacterium, *Pseudomonas*
1006 *chlororaphis* O6. Plant Pathol J 30: 215–219. https://doi.org/10.5423/PPJ.NT.11.2013.0109

1007 Kim, Y.K., and McCarter, L.L. (2000) Analysis of the polar flagellar gene system of *Vibrio*
1008 *parahaemolyticus*. J Bacteriol 188: 852-862. https://doi.org/10.1128/JB.182.13.3693-
1009 3704.2000

1010 Lacal, J., Reyes-Darías, J.A., García-Fontanas, C., Ramos, J.L., and Krell, T. (2013) Tactic
1011 responses to pollutants and their potential to increase biodegradation efficiency. J. Appl
1012 Microbiol 114: 923-933. https://doi.org/10.1111/jam.12076.

1013 Langmead, B., and Salzberg, S.L. (2012) Fast gapped-read alignment with Bowtie 2. Nat
1014 Meth 9: 357–359. https://doi.org/10.1038/nmeth.1923

1015 Li, H., Handsaker, B., Wysoker, A., Fennell, T., Ruan, J., Homer, N. *et al*. (2009) The
1016 Sequence Alignment/Map format and SAMtools. Bioinformatics 25: 2078–2079.

1017 https://doi.org/10.1093/bioinformatics/btp352

1018 Li, X.Z., Hauer, B., and Rosche, B. (2007) Single-species microbial biofilm screening for
1019 industrial applications. Appl Microbiol Biotechnol 76: 1255–1262.
1020 https://doi.org/10.1007/s00253-007-1108-4

1021 Llamas, M.A., Ramos, J.L., and Rodriguez-Herva, J.J. (2000) Mutations in each of the *tol*
1022 genes of *Pseudomonas putida* reveal that they are critical for maintenance of outer
1023 membrane stability. J Bacteriol 182: 4764–4772. https://doi.org/10.1128/JB.182.17.4764-
1024 4772.2000

1025 Ma, Y., Liu, Y., Bi, Y., Han, X., Jin, Y., Xu, H., and Qiao, M. (2021) OsaR (PA0056) functions
1026 as a repressor of the gene *fleQ* encoding an important motility regulator in *Pseudomonas*
1027 *aeruginosa* . J Bacteriol, in press. https://doi.org/10.1128/jb.00145-21

1028 Matilla, M.A., and Krell, T. (2021) The effect of bacterial chemotaxis on host infection and
1029 pathogenicity. FEMS Microbiol Rev 42: fux052. https://doi.org/10.1093/femsre/fux052.

1030 Markel, E., Dalenberg, H., Monteil, C.L., Vinatzer, B.A., and Swingle, B. (2018) An AlgU-
1031 regulated antisense transcript encoded within the *Pseudomonas syringae fleQ* gene has a
1032 positive effect on motility. J Bacteriol 200:e00576-17. https://doi.org/10.1128/JB.00576-17

1033 Martínez-García, E., and de Lorenzo, V. (2011) Engineering multiple genomic deletions in
1034 Gram-negative bacteria: Analysis of the multi-resistant antibiotic profile of *Pseudomonas*
1035 *putida* KT2440. Environ Microbiol 13: 2702–2716. https://doi.org/10.1111/j.1462-
1036 2920.2011.02538.x

1037 Martínez-García, E., and De Lorenzo, V. (2012) Transposon-based and plasmid-based
1038 genetic tools for editing genomes of Gram-negative bacteria. Methods Mol Biol 813: 267–
1039 283. https://doi.org/10.1007/978-1-61779-412-4_16

1040 Martínez-García, E., Nikel, P.I., Chavarría, M., and de Lorenzo, V. (2014) The metabolic
1041 cost of flagellar motion in *Pseudomonas putida* KT2440. Environ Microbiol 16: 291–303.

1042 https://doi.org/10.1111/1462-2920.12309

1043 Martínez-Granero, F., Navazo, A., Barahona, E., Redondo-Nieto, M., Rivilla, R., and Martín,
1044 M. (2012) The Gac-Rsm and SadB signal transduction pathways converge on AlgU to
1045 downregulate motility in *Pseudomonas fluorescens*. PLoS One 7: e31765
1046 https://doi.org/10.1371/journal.pone.0031765

1047 Martins Dos Santos, V.A.P., Heim, S., Moore, E.R.B., Strätz, M., and Timmis, K.N. (2004)
1048 Insights into the genomic basis of niche specificity of *Pseudomonas putida* KT2440. Environ
1049 Microbiol 6: 1264–1286. https://doi.org/10.1111/j.1462-2920.2004.00734.x

1050 McCarter, L.L. (2001) Polar Flagellar Motility of the Vibrionaceae . Microbiol Mol Biol Rev
1051 65: 445–462. https://doi.org/10.1128/mmbr.65.3.445-462.2001

1052 McDougald, D., Rice, S.A., Barraud, N., Steinberg, P.D., and Kjelleberg, S. (2012) Should
1053 we stay or should we go: Mechanisms and ecological consequences for biofilm dispersal.
1054 Nat Rev Microbiol 10: 39–50. https://doi.org/10.1038/nrmicro2695

1055 Miller, J.H. (1993) A short course in bacterial genetics - A laboratory manual and handbook
1056 for *Escherichia coli* and related bacteria. Cold Spring Harbor, New York, USA: Cold Spring
1057 Harbor Laboratory Press.

1058 Moisi, M., Jenul, C., Butler, S.M., New, A., Tutz, S., Reidl, J. *et al*. (2009) A novel regulatory
1059 protein involved in motility of *Vibrio cholerae*. J Bacteriol 191: 7027–7038.
1060 https://doi.org/10.1128/JB.00948-09

1061 Navarrete, B., Leal-Morales, A., Serrano-Ron, L., Sarrió, M., Jiménez-Fernández, A.,
1062 Jiménez-Díaz, L. *et al*. (2019) Transcriptional organization, regulation and functional
1063 analysis of *flhF* and *fleN* in *Pseudomonas putida*. PLoS One 14: e0214166.
1064 https://doi.org/10.1371/journal.pone.0214166

1065 Pallen, M.J., Penn, C.W., and Chaudhuri, R.R. (2005) Bacterial flagellar diversity in the post-
1066 genomic era. Trends Microbiol 13: 143–149. https://doi.org/10.1016/j.tim.2005.02.008

1067 Parkinson, J.S. (1976) *cheA*, *cheB*, and *cheC* genes of *Escherichia coli* and their role in
1068 chemotaxis. J Bacteriol 126: 758–770. https://doi.org/10.1128/jb.126.2.758-770.1976

1069 Petersen, B.D., Liu, M.S., Podicheti, R., Yang, A.Y.-P., Simpson, C.A., Hemmerich, C. *et al*.
1070 (2021) The polar flagellar transcriptional regulatory network in *Vibrio campbellii* deviates
1071 from canonical *Vibrio* species . J Bacteriol, in press. https://doi.org/10.1128/jb.00276-21

1072 Poggio, S., Osorio, A., Dreyfus, G., and Camarena, L. (2005) The flagellar hierarchy of
1073 *Rhodobacter sphaeroides* is controlled by the concerted action of two enhancer-binding
1074 proteins. Mol Microbiol 58: 969–983. https://doi.org/10.1111/j.1365-2958.2005.04900.x

1075 Prouty, M.G., Correa, N.E., and Klose, K.E. (2001) The novel σ^{54}- and σ^{28}-dependent
1076 flagellar gene transcription hierarchy of *Vibrio cholerae*. Mol Microbiol 39: 1595–1609.
1077 https://doi.org/10.1046/j.1365-2958.2001.02348.x

1078 Ringgaard, S., Yang, W., Alvarado, A., Schirner, K., and Briegel, A. (2018) Chemotaxis
1079 arrays in *Vibrio* species and their intracellular positioning by the ParC/ParP system. J
1080 Bacteriol 200: e00793. https://doi.org/10.1128/JB.00793-17

1081 Robinson, J.T., Thorvaldsdóttir, H., Winckler, W., Guttman, M., Lander, E.S., Getz, G., and
1082 Mesirov, J.P. (2011) Integrative genomics viewer. Nat Biotechnol 29: 24–26.
1083 https://doi.org/10.1038/nbt.1754

1084 Rodríguez-Herva, J.J., Duque, E., Molina-Henares, M A., Navarro-Avilés, G., van Dillewijn,
1085 P., de la Torre, J. *et al*. (2010) Physiological and transcriptomic characterization of a *fliA*
1086 mutant of *Pseudomonas putida* KT2440. Environ Microbiol Rep 2: 373–380.
1087 https://doi.org/10.1111/j.1758-2229.2009.00084.x

1088 Sambrook, J.E., and Russell, D.W. (2000) Molecular Cloning, a Laboratory Manual. Cold
1089 Spring Harbor, New York, USA: Cold Spring Harbor Laboratory Press.

1090 Sampedro, I., Parales, R.E., and Krell, T. (2015) *Pseudomonas* chemotaxis. FEMS
1091 Microbiol Rev 39: 17-46. https://doi.org/10.1111/1574-6976.12081.

1092 Schuhmacher, J.S., Rossmann, F., Dempwolff, F., Knauer, C., Altegoer, F., Steinchen, W.
1093 *et al*. (2015) MinD-like ATPase FlhG effects location and number of bacterial flagella during
1094 C-ring assembly. Proc Natl Acad Sci USA 112: 3092–3097.
1095 https://doi.org/10.1073/pnas.1419388112

1096 Schuhmacher, J.S., Thormann, K.M., and Bange, G. (2015) How bacteria maintain location
1097 and number of flagella?. FEMS MIcrobiol Rev 39: 812–822.
1098 https://doi.org/10.1093/femsre/fuv034

1099 Shi, M., Gao, T., Ju, L., Yao, Y., and Gao, H. (2014) Effects of FlrBC on flagellar biosynthesis
1100 of *Shewanella oneidensis*. Mol Microbiol 93: 1269–1283. https://doi.org/10.1111/mmi.12731

1101 Smith, T.G., and Hoover, T.R. (2009) Deciphering bacterial flagellar gene regulatory
1102 networks in the genomic era. Adv Appl Microbiol 67: 257-295.
1103 https://doi.org/10.1016/S0065-2164(08)01008-3

1104 Smith, T. G., Pereira, L., and Hoover, T. R. (2009) Helicobacter pylori FlhB processing-
1105 deficient variants affect flagellar assembly but not flagellar gene expression. Microbiology
1106 155(4), 1170–1180. https://doi.org/10.1099/mic.0.022806-0

1107 Sourjik, V., and Wingreen, N.S. (2012) Responding to chemical gradients: Bacterial
1108 chemotaxis. Curr Opin Cell Biol 24: 262–268. https://doi.org/10.1016/j.ceb.2011.11.008

1109 Tart, A.H., Blanks, M.J., and Wozniak, D.J. (2006) The AlgT-dependent transcriptional
1110 regulator AmrZ (AlgZ) inhibits flagellum biosynthesis in mucoid, nonmotile *Pseudomonas*
1111 *aeruginosa* cystic fibrosis isolates. J Bacteriol 188: 6483–6489.
1112 https://doi.org/10.1128/JB.00636-06

1113 Tart, A.H., Wolfgang, M.C., and Wozniak, D.J. (2005) The alternative sigma factor AlgT
1114 represses *Pseudomonas aeruginosa* flagellum biosynthesis by inhibiting expression of fleQ.
1115 J Bacteriol 187: 7955–7962. https://doi.org/10.1128/JB.187.23.7955-7962.2005

1116 Terashima, H., Kojima, S., and Homma, M. (2008) Flagellar motility in bacteria. Structure

1117 and function of flagellar motor. Int Rev Cell Mol Biol 270: 39-85.
1118 https://doi.org/10.1016/S1937-6448(08)01402-0

1119 Toutain, C.M., Zegans, M.E., and O'Toole, G.A. (2005) Evidence for two flagellar stators
1120 and their role in the motility of *Pseudomonas aeruginosa*. J Bacteriol 187: 771–777.
1121 https://doi.org/10.1128/JB.187.2.771-777.2005

1122 Tsang, J., and Hoover, T.R. (2015) Basal body structures differentially affect transcription of
1123 RpoN and FliA-dependent flagellar genes in *Helicobacter pylori*. J Bacteriol 197: 1921–
1124 1930. https://doi.org/10.1128/JB.02533-14

1125 Valentini, M., Laventie, B.J., Moscoso, J., Jenal, U., and Filloux, A. (2016) The diguanylate
1126 cyclase HsbD intersects with the HptB regulatory cascade to control *Pseudomonas*
1127 *aeruginosa* biofilm and motility. PLoS Genet 12: e1006354
1128 https://doi.org/10.1371/journal.pgen.1006354

1129 Vera, J.M., Ghosh, I.N., Zhang, Y., Hebert, A.S., Coon, J.J., and Landick, R. (2020)
1130 Genome-scale transcription-translation mapping reveals features of *Zymomonas mobilis*
1131 transcription units and promoters. mSystems 5: e00250-20.
1132 https://doi.org/10.1128/msystems.00250-20

1133 Wand, M.E., Sockett, R.E., Evans, K.J., Doherty, N., Sharp, P.M., Hardie, K.R., and Winzer,
1134 K. (2006) *Helicobacter pylori* FlhB function: The FlhB C-terminal homologue HP1575 acts
1135 as a "spare part" to permit flagellar export when the HP0770 FlhBCC domain is deleted. J
1136 Bacteriol 188: 7531–7541. https://doi.org/10.1128/JB.00263-06

1137 Wang, Y., Li, Y., Wang, J., and Wang, X. (2018) FleQ regulates both the type VI secretion
1138 system and flagella in *Pseudomonas putida*. Biotechnol Appl Chem 65: 419–427.
1139 https://doi.org/10.1002/bab.1611

1140 Warrier, I., Ram-Mohan, N., Zhu, Z., Hazery, A., Echlin, H., Rosch, J. *et al*. (2018) The
1141 Transcriptional landscape of *Streptococcus pneumoniae* TIGR4 reveals a complex operon

1142 architecture and abundant riboregulation critical for growth and virulence. PLoS PAthog 14:
1143 e1007461. https://doi.org/10.1371/journal.ppat.1007461

1144 Wilhelms, M., Molero, R., Shaw, J.G., Tomás, J. M., and Merino, S. (2011) Transcriptional
1145 hierarchy of *Aeromonas hydrophila* polar-flagellum genes. J Bacteriol 193: 5179–5190.
1146 https://doi.org/10.1128/JB.05355-11

1147 Winsor, G.L., Griffiths, E.J., Lo, R., Dhillon, B.K., Shay, J.A., and Brinkman, F.S.L. (2016)
1148 Enhanced annotations and features for comparing thousands of *Pseudomonas* genomes in
1149 the *Pseudomonas* genome database. Nucleic Acids Res 44: D646–D653.
1150 https://doi.org/10.1093/nar/gkv1227

1151 Wirebrand, L., Österberg, S., López-Sánchez, A., Govantes, F., and Shingler, V. (2018)
1152 PP4397/FlgZ provides the link between PP2258 c-di-GMP signalling and altered motility in
1153 *Pseudomonas putida*. Sci Rep 8: 12205. https://doi.org/10.1038/s41598-018-29785-w

1154 Wu, L., Wang, J., Tang, P., Chen, H., and Gao, H. (2011) Genetic and molecular
1155 characterization of flagellar assembly in *Shewanella oneidensis*. PLoS One 6: e21479.
1156 https://doi.org/10.1371/journal.pone.0021479

1157 Yan, B., Boitano, M., Clark, T.A., and Ettwiller, L. (2018) SMRT-Cappable-seq reveals
1158 complex operon variants in bacteria. Nat Commun 9: 3676. https://doi.org/10.1038/s41467-
1159 018-05997-6

1160 Zhou, T., Huang, J., Liu, Z., Xu, Z., and Zhang, L. (2021) Molecular mechanisms underlying
1161 the regulation of biofilm formation and swimming motility by FleS/FleR in *Pseudomonas*
1162 *aeruginosa*. Front Microbiol 12: 707711. https://doi.org/10.3389/fmicb.2021.707711

1163

1164 **FIGURE LEGENDS**

1165 **Figure 1. The *Pseudomonas* flagellar cluster.** Synteny relationships between the 59
1166 flagella-related genes in the *Pseudomonas* flagellar cluster. Genes are color-coded to
1167 denote their putative function as indicated. **A.** Cartoon of the *P. putida* KT2440 flagellar
1168 cluster, including designations of all 59 flagella-related genes and the 20 promoters
1169 identified in this work. The 7-gene insertion (PP_4345 to PP_4351) upstream from *flhA* is
1170 omitted (indicated by two oblique lines). **B.** Simplified cartoons of the *Pseudomonas* Group
1171 I, II, III and IV flagellar clusters. Dashed lines indicate points of synteny disruption between
1172 groups. Black arrows indicate preferential locations for insertion of small groups of additional
1173 genes.

1174 **Figure 2. RNA-seq and RT-PCR analysis of the transcriptional organization of the *P.***
1175 ***putida* KT2440 flagellar cluster. A.**, **C.** and **E.** Output of the RNA-seq analysis of the
1176 KT2440 flagellar cluster, split in three regions. Coverage is represented in grey on a
1177 logarithmic scale. Top strand and bottom strand reads are shown in blue and pink,
1178 respectively. **B.**, **D.** and **F.** Agarose gel electrophoresis showing the RT-PCR results for
1179 selected regions of the *flhAF-fleN-flhF-fliA-cheYZAB-motCD-parCP-cheW-flrD* (**B**), *hsbAR-*
1180 *hptB-fliKLMNOPQR-flhB*, *fliEFG and fliHIJ* (**C**) and *fliC-flaG-fliDST-fleQSR* (**F**) operons. Plus
1181 (+) and minus (-) signs denote PCR reactions performed with genomic DNA and RNA,
1182 respectively, as templates. A cartoon of the flagellar genes is aligned with the RNA-seq
1183 reads and RT-PCR results. Genes are color-coded as in **Fig. 1.** An inverted triangle denotes
1184 the location of the *flhF*::miniTn*5*-Km insertion. The RNA-seq images represent data from a
1185 single representative replicate. Each RT-PCR image was cropped from a single picture and
1186 represents consecutive lanes of a representative agarose gel.

1187 **Figure 3. The *P. putida* KT2440 flagellar promoter set.** Sequences of the twenty-one
1188 putative *P. putida* KT2440 flagellar promoters identified in this work, along with the
1189 consensus sequences for the corresponding σ factors: σ^{54} (**A**), FliA (**B**) and σ^{70} (**C**). The

1190 promoter motifs are indicated in red, and the coding sequences of the upstream genes are
1191 indicated in blue.

1192 **Figure 4. Expression of the P*fleQ* and P*fliH* promoters in *P. putida* KT2442 and mutant**
1193 **derivatives.** β-galactosidase assays of the P*fleQ* (**B**) and P*fliH* (**B**) promoter fusions in the
1194 wild-type strain KT2442 and its Δ*fleQ*, Δ*fleN*, Δ*fleR*, Δflagella and Δflagella ectopically
1195 expressing FleQ or FliA derivatives. **Ø** denotes no further modification of the genetic
1196 background indicated below. Bars represent the averages and standard deviations of at
1197 least three independent assays. Stars designate p-values for the Student's t-test for
1198 unpaired samples not assuming equal variance. ns: $p \geq 0.05$; *: $p<0.05$; **: $p<0.01$;
1199 ***:$p<0.001$. For each promoter fusion, the T-test was performed for (i) empty vector *vs.*
1200 promoter fusion in the wild-type strain; (ii) the wild-type *vs* the set of deletion mutants, (iii)
1201 the Δflagella mutant *vs.* its derivatives producing FleQ or FliA; and (iv) each fusion-bearing
1202 strain in exponential *vs.* stationary phase.

1203 **Figure 5. Expression the Class II flagellar promoters in *P. putida* KT2442 and mutant**
1204 **derivatives.** Differential rates of GFP fluorescence accumulation of the P*parC* (**A**), P*flhF*
1205 (**B**), P*flhA* (**C**), P*fliL* (**D**), P*fliK*(**E**), P*fliE* (**F**), P*fleS* (**G**), P*fliD* (**H**), P*flgF* (**I**), P*flgB* (**J**), P*flgA* (**K**)
1206 and P*flgZ* (**L**) promoters in the wild-type strain KT2442 and its Δ*fleQ*, Δ*rpoN*, Δ*fleN*, Δ*fleR*,
1207 Δflagella, Δflagella ectopically expressing FleQ or FliA, and *lapA*$^-$ expressing YhjH or PleD
1208 derivatives. **Ø** denotes no further modification of the genetic background indicated below.
1209 Bars represent the averages and standard deviations of at least three independent assays.
1210 Stars designate p-values for the Student's t-test for unpaired samples not assuming equal
1211 variance. Results are shown for the pairwise comparisons of the Δ*fleQ*, Δ*rpoN*, Δ*fleN* and
1212 Δ*fleR* mutants using the wild-type strain as the reference, the Δflagella strain expressing
1213 FleQ or FliA using the Δflagella strain as a reference, and all pairwise comparisons involving
1214 the *lapA*- mutant and its derivatives expressing YhjH or PleD. ns: $p \geq 0.05$; *: $p<0.05$; **:
1215 $p<0.01$; ***:$p<0.001$. The complete statistical analysis of this dataset is available in
1216 **Supplementary File S3**.

1217 **Figure 6. Expression the Class III flagellar promoters in *P. putida* KT2442 and mutant**
1218 **derivatives.** Differential rates of GFP fluorescence accumulation of the P*fliK2* (**A**), P*cheA*
1219 (**B**), P*hsbA* (**C**), P*fliS* (**D**), P*fliC*(**E**), P*cheV* (**F**), P*flgM* (**G**) and P*motA* (**H**) promoters in the
1220 wild-type strain KT2442 and its Δ*fleQ*, Δ*rpoN*, Δ*fleN*, Δ*fleR*, Δflagella and Δflagella ectopically
1221 expressing FleQ or FliA. **Ø** denotes no further modification of the genetic background
1222 indicated below. Bars represent the averages and standard deviations of at least three
1223 independent assays. Stars designate p-values for the Student's t-test for unpaired samples
1224 not assuming equal variance. Results are shown for the pairwise comparisons of the Δ*fleQ*,
1225 Δ*rpoN*, Δ*fleN* and Δ*fleR* mutants using the wild-type strain as the reference, and the Δflagella
1226 strain expressing FleQ or FliA using the Δflagella strain as a reference. ns: $p \geq 0.05$; *: $p<0.05$;
1227 **: $p<0.01$; ***:$p<0.001$. The complete statistical analysis of this dataset is available in
1228 **Supplementary File S3**.
1229 **Figure 7. Hypothetical model of the flagellar transcriptional cascade in *P. putida***
1230 **KT2440.** Cartoon representing the transcriptional hierarchy, feed-forward and feedback
1231 loops of the *P. putida* KT2440 flagellar cascade. Genes are shaded in grey, transcription
1232 factors are shaded in pink, σ factors are shaded in purple. and auxiliary regulatory proteins
1233 are shaded in orange. Transcription is shown as green arrows and translation is shown as
1234 black dashed arrows. Green dashed arrows and red dashed lines with a round end denote
1235 positive and regulatory events based on protein-protein interaction, respectively. FlgM
1236 secretion by way of the FT3SS is denoted by a dashed grey arrow. Three stages of flagellar
1237 assembly are represented: early basal body (EBB), the hook-basal body complex (HBB),
1238 and the complete flagellum.
1239
1240

1241 **SUPPORTING MATERIALS LEGENDS**

1242 **Supplementary File S1. Synteny analysis of the flagellar cluster in 401 *Pseudomonas***
1243 **genomes.** Each of the four groups is shown in a separate tabs. The values indicate the
1244 number of intervening genes between each of the gene pairs above in each genome. Yellow
1245 frames indicate the flagellar operons of *P. putida* KT2440. Absent genes are denoted by an
1246 X.

1247 **Supplementary File S2. Sequence alignments of the flagellar promoter regions in**
1248 **seven environmental *Pseudomonas* strains.** Output of the MUSCLE alignment in
1249 CLUSTALW format. PpuKT2440: *P. putida* KT2440; PpuF1: *P. putida* F1; PsyDC3000: *P.*
1250 *syringae* pv tomato DC3000; PsyB728a: *P. syringae* pv syringae B728a; Psa1448a: *P.*
1251 *savatanoi* 1448a; PflSBW25: *P. fluorescens* SBW25; PprPF5: *P. protegens* PF5. Asterisks
1252 indicate positions conserved in all seven strains. Coding sequences are shown in blue, and
1253 putative promoter motifs are shown in red.

1254 **Supplementary File S3. Statistical analysis of the differential rate of fluorescence**
1255 **accumulation dataset represented in Figs. 5 and 6.** The average, standard deviation, the
1256 numerical and symbol representation of the T-test results and the fold difference in pairwise
1257 comparisons are shown for each combination of promoter fusion and genetic background.
1258 Fold differences are positive when expression is greater in the reference strain and negative
1259 when expression is smaller in the reference strain. Lines are color-coded as follows. Green:
1260 statistically significant difference, fold change greater than 2; yellow: statistically significant
1261 difference, fold change smaller than 2; red: difference not statistically significant.

1262 **Supplementary Table S1. Inventory of flagellar genes *P. putida* KT2440 flagellar**
1263 **cluster.** *P. putida* locus tags are according to the TIGR sequencing project annotation
1264 available at the *Pseudomonas* Genome Database (pseudomonas.com). Putative functions
1265 are based on experimental evidence obtained in *P. putida* or other organisms.

1266 **Supplementary Table S2. Class II flagellar gene expression in *Escherichia coli*.** The
1267 values show β-galactosidase activity (Miller units) stationary phase cultures of *E. coli*

1268 ET8000 bearing the empty vector pSB1K3, or pMRB99, expressing *P. putida* KT2440 FleQ
1269 from its own promoter grown in LB. Also shown are the number of biological replicates (n)
1270 for each fusion and strain, the averages and standard deviations, the fold differences
1271 (ET8000/pMRB99 / ET8000/pSB1K3 ratio) in the β-galactosidase activity and the T-test *p*-
1272 values are shown. ns: $p \geq 0.05$*; = $p<0.05$; ** = $p<0.01$; *** = $p<0.001$.

1273 **Supplementary Table S3. Effect of *rpoN* deletion on Class II flagellar gene expression.**
1274 The values show β-galactosidase activity (Miller units) from exponential and stationary
1275 phase cultures of *P. putida* KT2442 (wild-type) and MRB149 (Δ*rpoN*) grown in LB containing
1276 10 mM glutamine. The number of biological replicates (n) for each fusion and strain, the
1277 averages and standard deviations, the fold differences (wild-type/Δ*rpoN* ratio) in the β-
1278 galactosidase activity and the T-test *p*-values are shown. ns: $p \geq 0.05$*; = $p<0.05$; ** = $p<0.01$;
1279 *** = $p<0.001$.

1280 **Supplementary Table S4. Bacterial strains, plasmids and oligonucleotides used in**
1281 **this work.** Underlined bases indicate oligonucleotide positions that differ from the
1282 corresponding templates. [1]Reference list for this Table shown as Supplementary
1283 References below.

1284 **Supplementary Figure S1. RNA-seq analysis of the *motAB* operon.** Output of the RNA-
1285 seq analysis of the genomic region containing the *motAB* operon. Coverage is represented
1286 in grey on a logarithmic scale. Top strand and bottom strand reads are shown in blue and
1287 pink, respectively. A cartoon of the flagellar genes is aligned with the RNA-seq reads. Genes
1288 are color-coded as in **Fig. 1**.

1289 **Supplementary Figure S2. Identification of putative flagellar promoters.** Sequences
1290 from the upstream regions of selected flagellar genes from *P. putida* KT2440 and F1, *P.*
1291 *syringae* DC3000 and B728a, *P. savastanoi* 1448a, *P. fluorescens* SBW25 and *P. protegens*
1292 Pf-5 with the putative promoters aligned along with the established consensus for σ^{54}, FliA
1293 and σ^{70}-dependent promoters. No gaps are introduced, except when required for alignment

1294 of the promoter motifs. Promoter sequences are indicated in red and coding sequences of
1295 the upstream genes are indicated in blue.

1296 **Supplementary Figure S3. An example of the GFP fluorescence vs. absorbance plot.**
1297 Fluorescence data collected along the growth curves of the wild-type (red) and Δ*fleQ* (blue)
1298 strains bearing the P*flgB-gfp-lacZ* fusion plasmid pMRB272 were plotted against the A_{600}
1299 data. Circles, squares and triangles denote three independent biological replicates, with the
1300 darker colors denoting the data used for the linear regression and the lighter colors denoting
1301 those not used. Dotted lines denote the linear fit obtained for the selected data of each
1302 replicate.

1303 **Supplementary Figure S4. RT-PCR of *fleQ* expressed from its natural genomic context**
1304 **and ectopically.** Ethidium bromide-stained 1% agarose electrophoresis gel showing the
1305 amplification reaction products obtained with *fleQ*-specific (lanes 1-5) and *fliT*-specific (lanes
1306 6-10) oligonucleotides. The template DNA was KT2442 genomic DNA (lanes 1 and 6),
1307 KT2442 cDNA (lanes 2 and 7), MRB130(Δflagella) cDNA (lanes 3 and 8), or
1308 MRB130/miniTn*7-nahR*-P*sal-fleQ* cDNA (lanes 4 and 9). Lanes 5 and 10 contain reactions
1309 performed with no template DNA. The picture shows one representative result of three
1310 biological replicates.

1311 **Supplementary Figure S5. Putative FleQ binding sites at the Class II promoter**
1312 **regions. A.** Cartoon of each Class II promoter region showing the putative s54 promoter in
1313 red and the putative FleQ binding sites in green, along with the distances between the
1314 different *cis*-acting elements. **B. and C.** The putative FleQ binding sites, aligned, and the
1315 logo derived from the sequences of these sites using WebLogo 3.7.4. (Crooks *et al*., 2004)
1316 (+) and (-) indicate the orientation of the sequences as shown in **B.** relative to the promoter
1317 (coding and non-coding strand, respectively).

1318 **Supplementary Figure S6. Swimming assay of the Δ*fleR* and Δ*fleS* mutants.** Swimming
1319 halos obtained in tryptone-soft agar plates with the wild-type strain KT2442 and its Δ*fleQ*,
1320 Δ*fleR* and Δ*fleS* derivatives. The images show representative halos from identical plates

1321 grown in parallel in the same conditions. Cropping was performed maintaining the scale of
1322 the respective images.

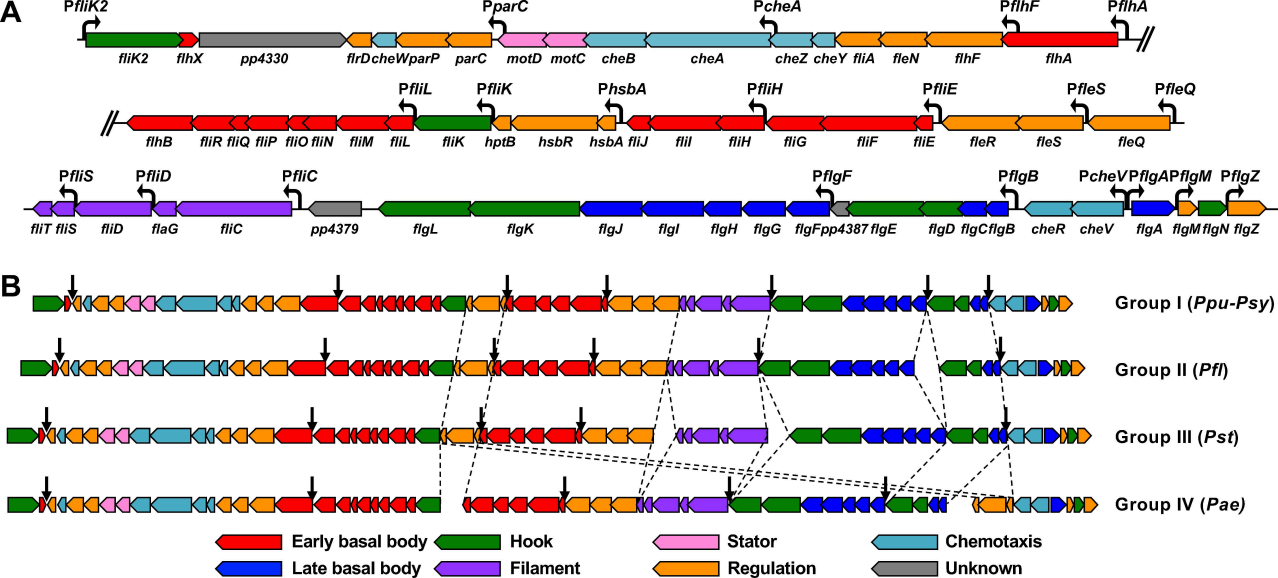
A
PfliK2
PparC
PcheA
PflhF
PflhA
fliK2 flhX pp4330 flrD cheW parP parC motD motC cheB cheA cheZ cheY fliA fleN flhF flhA
PfliL
PfliK
PhsbA
PfliH
PfliE
PfleS
PfleQ
flhB fliR fliQ fliP fliO fliN fliM fliL fliK hptB hsbR hsbA fliJ fliI fliH fliG fliF fliE fleR fleS fleQ
PfliS
PfliD
PfliC
PflgF
PflgB
PcheV
PflgA
PflgM
PflgZ
fliT fliS fliD flaG fliC pp4379 flgL flgK flgJ flgI flgH flgG flgF pp4387 flgE flgD flgC flgB cheR cheV flgA flgM flgN flgZ
B
Group I (Ppu-Psy)
Group II (Pfl)
Group III (Pst)
Group IV (Pae)
Early basal body
Hook
Stator
Chemotaxis
Late basal body
Filament
Regulation
Unknown

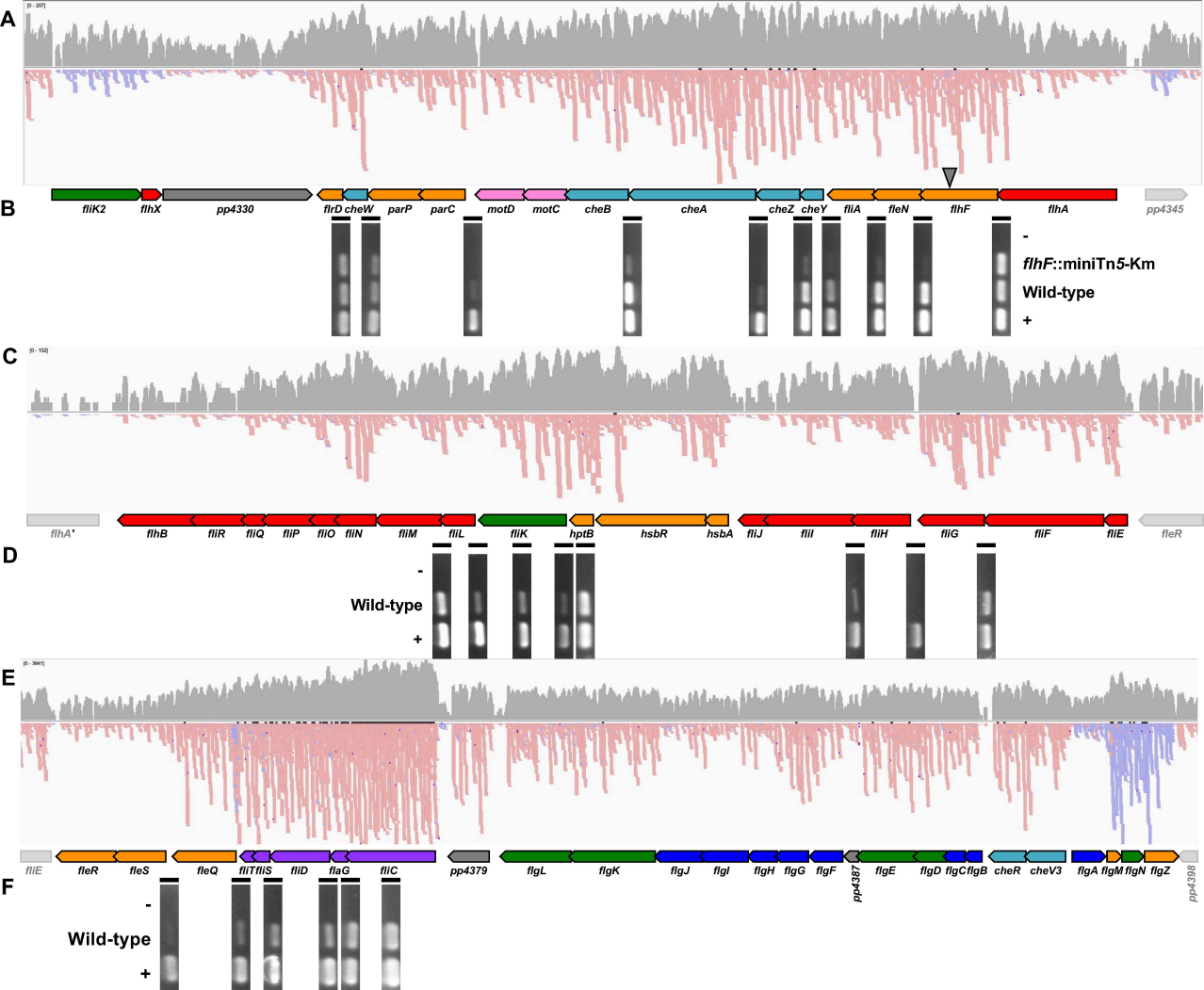
A
B
fliK2
flhX
pp4330
flrD
cheW
parP
parC
motD
motC
cheB
cheA
cheZ
cheY
fliA
fleN
flhF
flhA
pp4345
-
flhF::miniTn5-Km
Wild-type
+
C
flhA'
flhB
fliR
fliQ
fliP
fliO
fliN
fliM
fliL
fliK
hptB
hsbR
hsbA
fliJ
fliI
fliH
fliG
fliF
fliE
fleR
D
-
Wild-type
+
E
fliE
fleR
fleS
fleQ
fliT
fliS
fliD
flaG
fliC
pp4379
flgL
flgK
flgJ
flgI
flgH
flgG
flgF
pp4387
flgE
flgD
flgC
flgB
cheR
cheV3
flgA
flgM
flgN
flgZ
pp4398
F
-
Wild-type
+

A

σ^{54} consensus

TGGCACG–N_4– TTGCw

PparC	TGCGCCGGGC**TGGCACA**CAAA**GTGCA**CCGGCAATAC
PflhF	GAGCCAAGGT**TGGAACA**GATT**TTGCT**GAATAGTCTG
PflhA	CTGCCAAAGT**TGGAAAG**CTTC**TTGCA**AAGCCACGCC
PfliL	CTGCAAAATC**TGGCATA**ACAC**TTGCT**CAAGCCAAGC
PfliK	**A**TACGCGAGT**TGGCGCG**AGTC**TTGCC**TGTCTCTGCC
PfliE	TTGCGAAGGC**TGGCACC**TTTG**TTGCT**TTAGGTAGGT
PfleS	CCCCCATCTC**CGGCACG**GCTA**TTGCT**ACACCGCTGG
PfliD	TGTG**TAA**TGT**TGGCATG**AGTCTTGACTCGGATTGTG
PflgF	GTTTCAGACT**TGGTTCA**ATTA**TTGCT**TGGAACCTGC
PflgB	TTCCAGTGGT**TGGCACA**GCCC**TTGCT**ATGCCTTGCT
PflgA	GGTAGCGAGT**CGGCACG**GGCT**TTGCT**TTTTTGAGTG
PflgZ	CAGAACATAG**TGGCAAA**ATGCCGTTACTTGCGTGTG

B

FliA consensus

TcAAgNw —N_{12-13}– gcCGAtaNc

PfliK2	CCCTTGTGTC**TCAAGTC**GCCCCG-CGCGCT**GCCGTTATA**CTGGCAACCA
PcheA	CGACTCGGGG**TGAAGGT**CCGCAG-ATTCAT**GCCGATAAG**CGTGAAGACG
PfliS	**A**TGGTCGTAT**TCAAGAT**CTTTGG-GGCTAA**GCCGATCAC**TTAGGTATGT
PfliC	GAAAAAACCC**TCAAGCA**ACCCGC-GCACCC**GACGATAAC**CATTACGAAG
PcheV	AACGGTGAAT**TCAAGAA**ACCCTTGGGTGAC**ACCGATAAG**CTGTTCAGGC
PflgM	CATTTGTGCC**TAAAGTT**TATATC-GGGTTG**GCCGAAAAC**AAGGCAAGCG
PmotA	ATTGAGTGGC**TATAGTC**TGGCGC AGTTCT**GCCGATAAG**TAGAAGAAGA

C

σ^{70} consensus (extended -10)

TTGACA –N_{14-15}– TGNTATAaT

PhsbA	CTGCATCCGC**TTGCCT**CCCCCACCATCGCC**TGCTAAACC**TTAAAGCAGT
PfleQ	CGCCATAAAT**TTGACT**GCCTTTAAGTTTTTGAC**TTTACT**AGTGGCTGTT

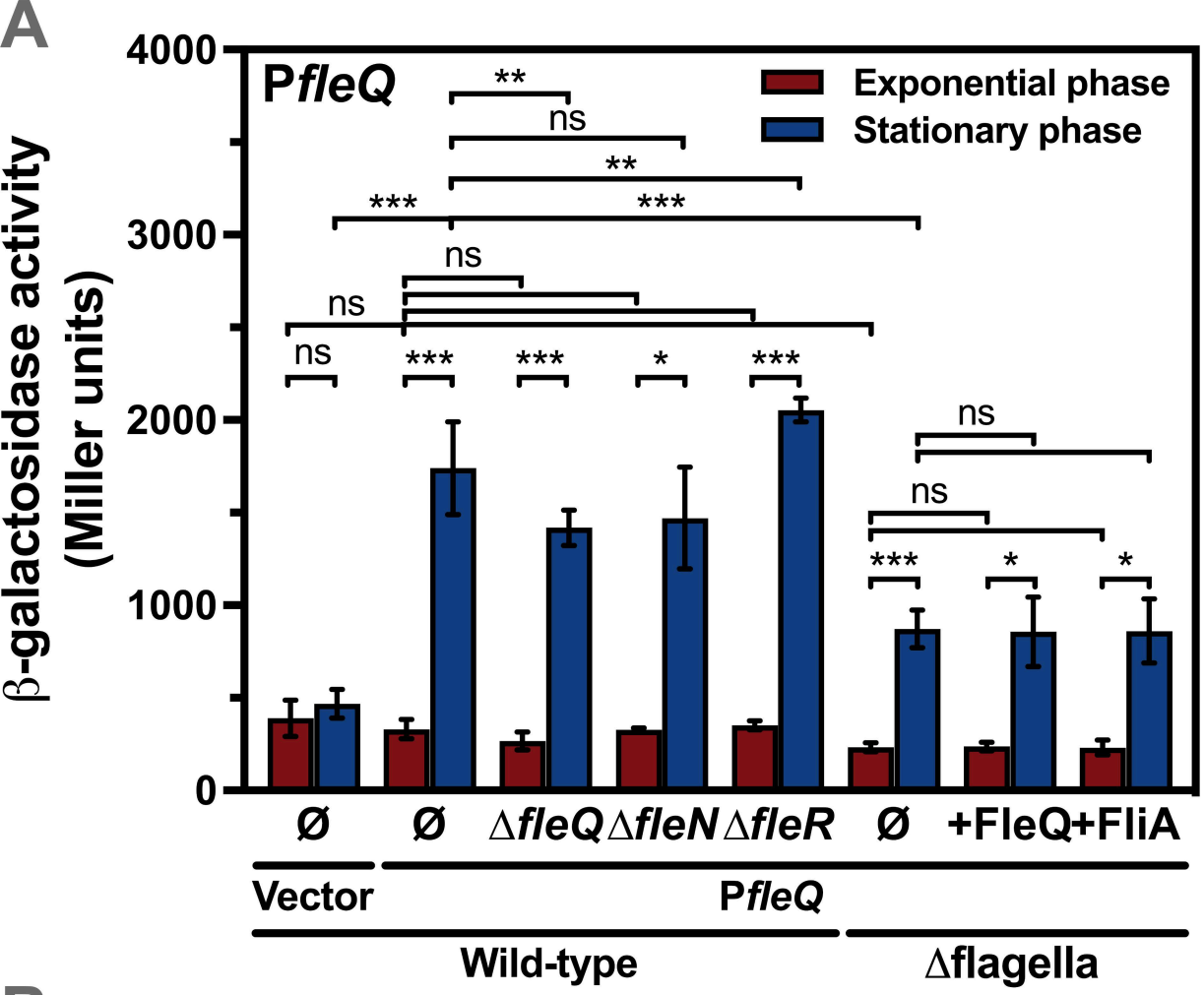
A
PfleQ
Exponential phase
Stationary phase
β-galactosidase activity (Miller units)
4000
3000
2000
1000
0
**
ns
**
***
***
ns
ns
ns
***
***
*
***
ns
ns
***
*
*
Ø
Ø
ΔfleQ
ΔfleN
ΔfleR
Ø
+FleQ+FliA
Vector
PfleQ
Wild-type
Δflagella

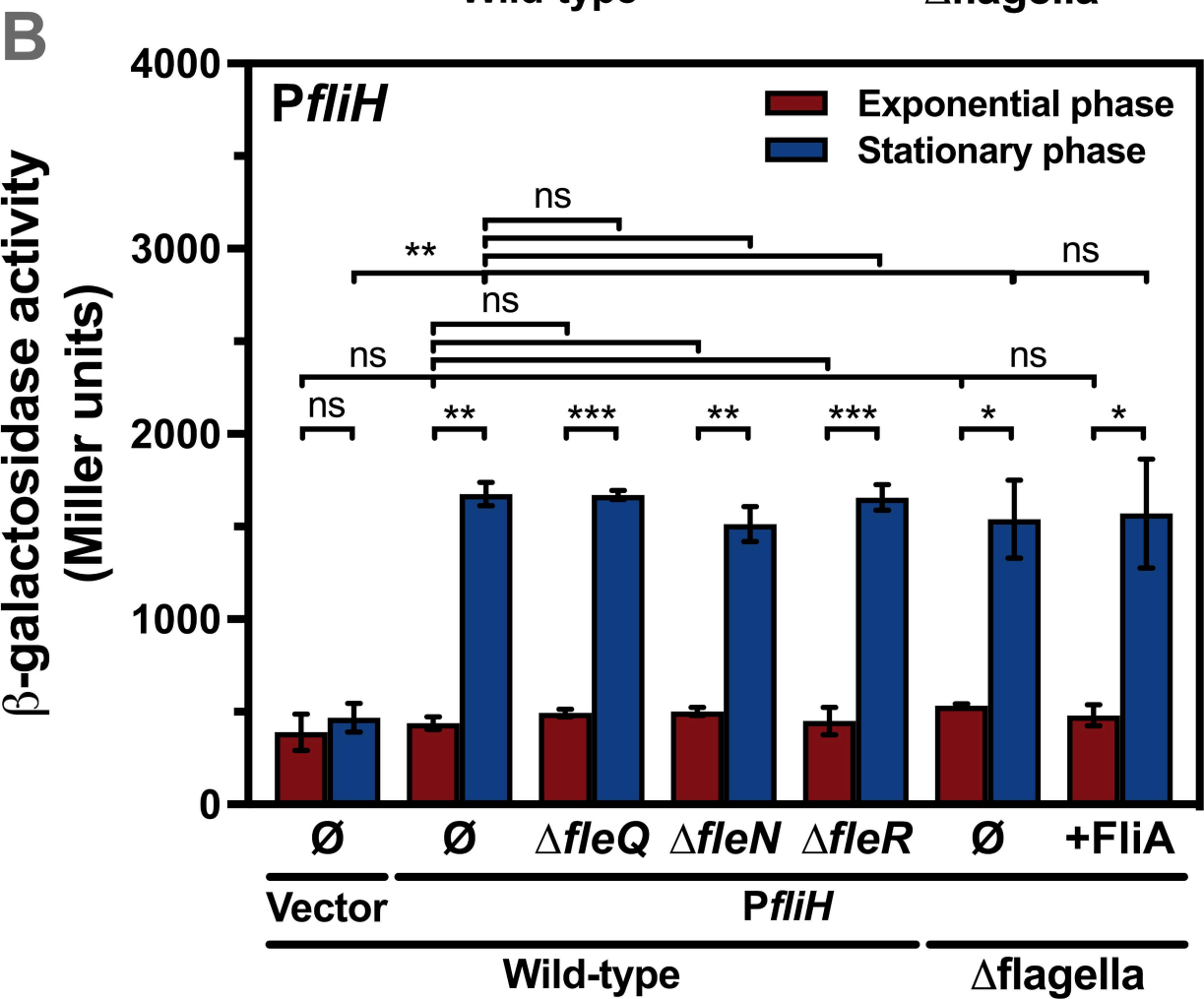
B
PfliH
Exponential phase
Stationary phase
β-galactosidase activity (Miller units)
4000
3000
2000
1000
0
ns
**
ns
ns
ns
ns
ns
**
***
**
***
*
*
Ø
Ø
ΔfleQ
ΔfleN
ΔfleR
Ø
+FliA
Vector
PfliH
Wild-type
Δflagella

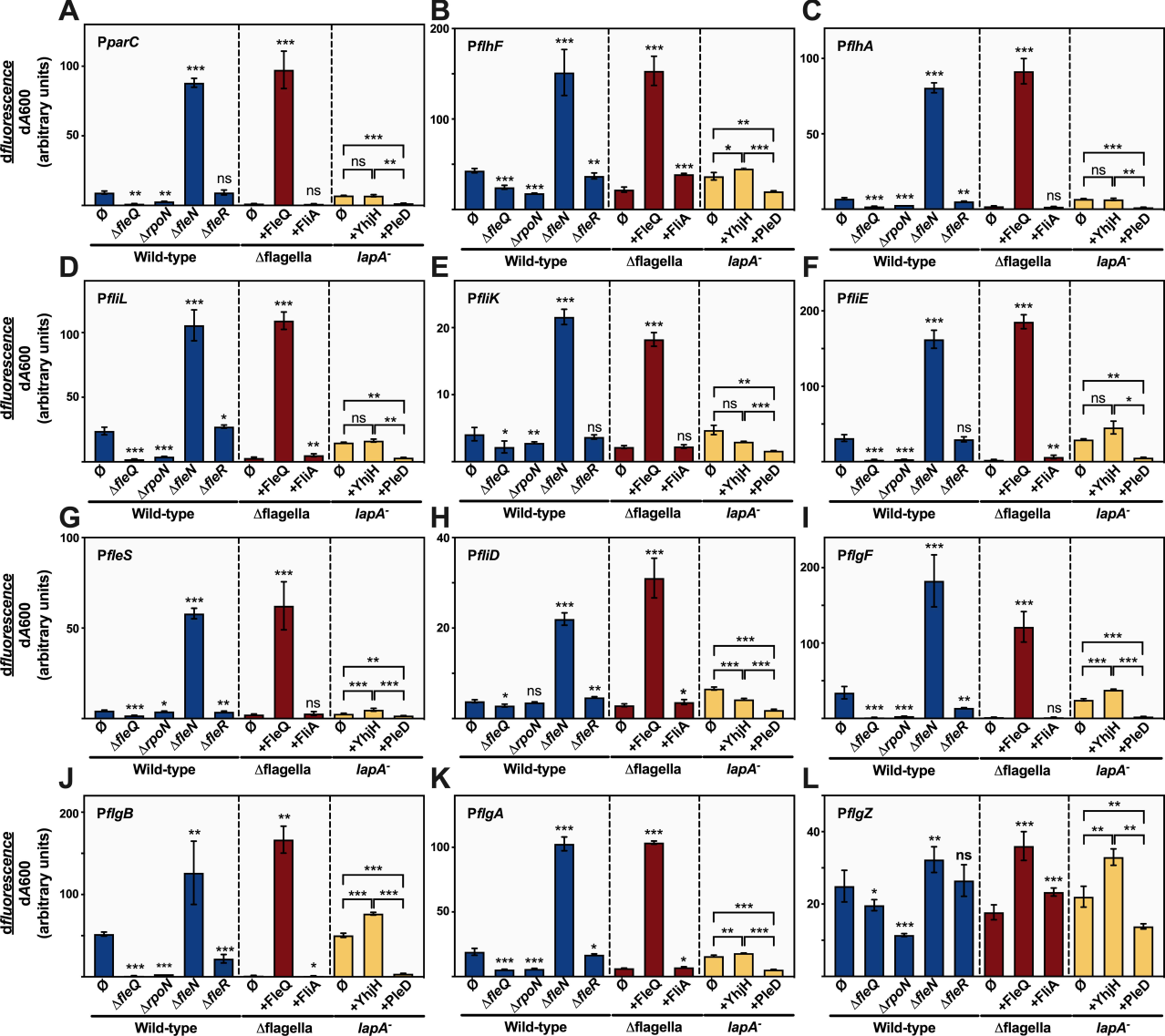
A
PparC
B
PflhF
C
PflhA
D
PfliL
E
PfliK
F
PfliE
G
PfleS
H
PfliD
I
PflgF
J
PflgB
K
PflgA
L
PflgZ
dfluorescence
dA600
(arbitrary units)
Ø
ΔfleQ
ΔrpoN
ΔfleN
ΔfleR
+FleQ
+FliA
+YhjH
+PleD
Wild-type
Δflagella
lapA-
ns

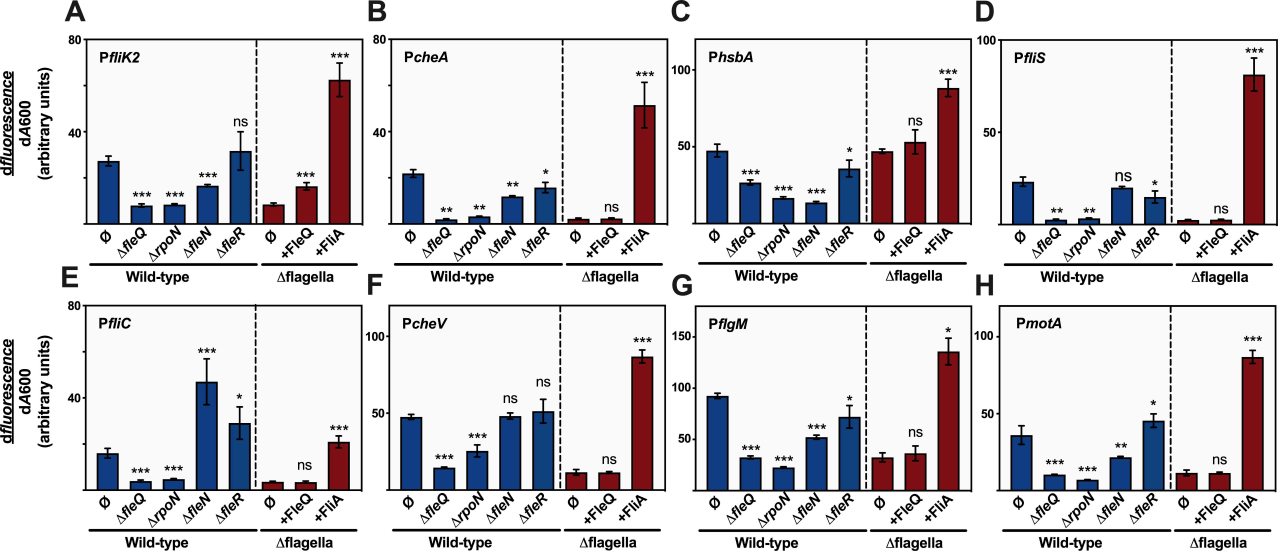
A
B
C
D
E
F
G
H
dfluorescence
dA600
(arbitrary units)
PfliK2
PcheA
PhsbA
PfliS
PfliC
PcheV
PflgM
PmotA
Ø
ΔfleQ
ΔrpoN
ΔfleN
ΔfleR
+FleQ
+FliA
Wild-type
Δflagella
***
**
*
ns

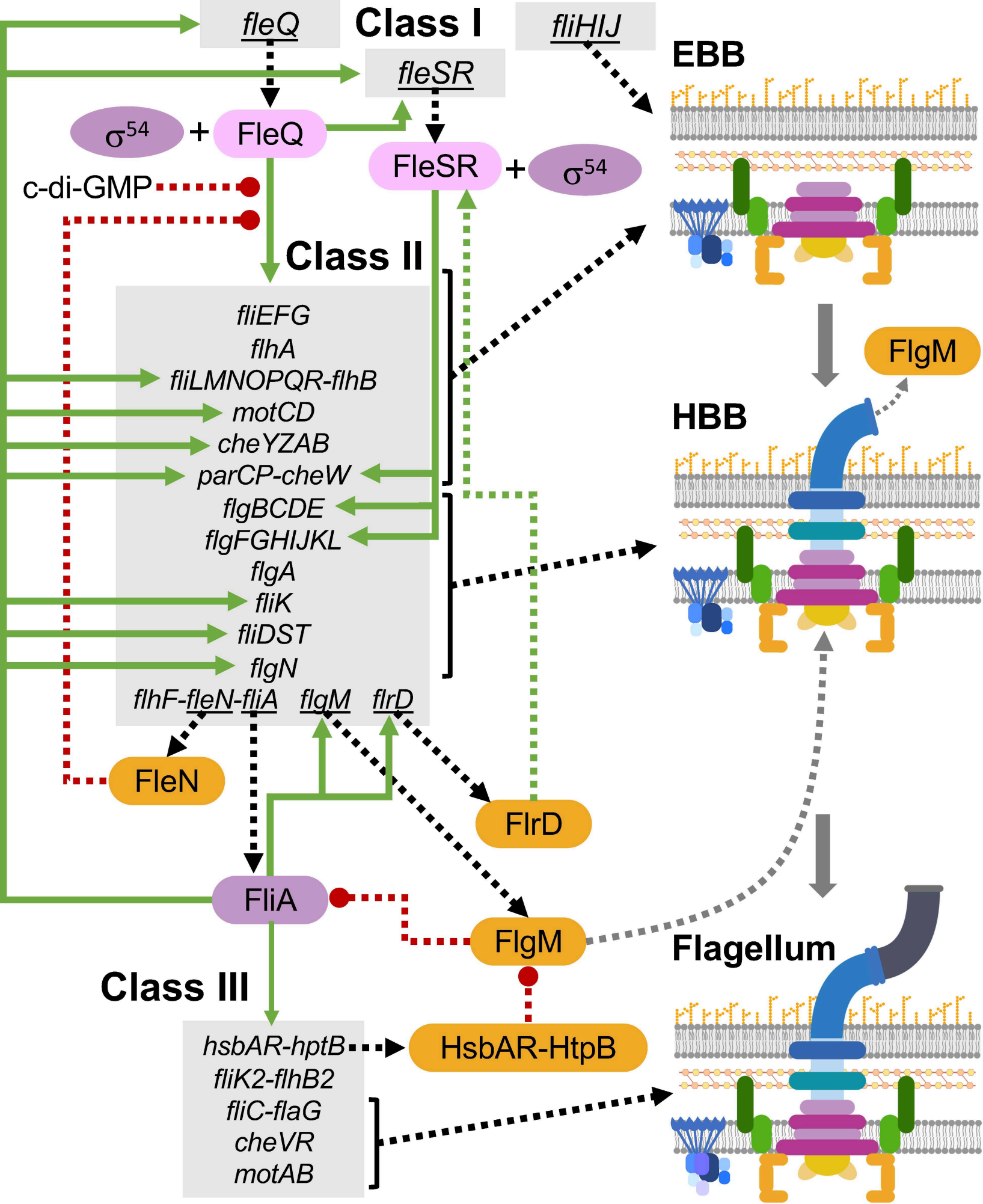
fleQ
Class I
fliHIJ
fleSR
EBB
σ54
+
FleQ
FleSR
+
σ54
c-di-GMP
Class II
fliEFG
flhA
fliLMNOPQR-flhB
motCD
cheYZAB
parCP-cheW
flgBCDE
flgFGHIJKL
flgA
fliK
fliDST
flgN
flhF-fleN-fliA
flgM
flrD
FlgM
HBB
FleN
FlrD
FliA
FlgM
Flagellum
Class III
hsbAR-hptB
fliK2-flhB2
fliC-flaG
cheVR
motAB
HsbAR-HtpB